



JRC SCIENTIFIC AND POLICY REPORTS

# Physical Characterization of Exhaust Particle Emissions from Late Technology Gasoline Vehicles

Authors:

Athanasios Mamakos, Urbano Manfredi

Editors:

Giorgio Martini, Adolfo Perujo, Alessandro Marotta

2012

European Commission  
Joint Research Centre  
Institute for Energy and Transport

Contact information

Forename Surname

Address: Joint Research Centre, Via Enrico Fermi 2749, TP xxx, 21027 Ispra (VA), Italy

E-mail: [giorgio.martini@jrc.ec.europa.eu](mailto:giorgio.martini@jrc.ec.europa.eu)

Tel.: +39 0332 789293

<http://iet.jrc.ec.europa.eu/>

<http://www.jrc.ec.europa.eu/>

This publication is a Reference Report by the Joint Research Centre of the European Commission.

Legal Notice

Neither the European Commission nor any person acting on behalf of the Commission is responsible for the use which might be made of this publication.

Europe Direct is a service to help you find answers to your questions about the European Union

Freephone number (\*): 00 800 6 7 8 9 10 11

(\*): Certain mobile telephone operators do not allow access to 00 800 numbers or these calls may be billed.

A great deal of additional information on the European Union is available on the Internet.

It can be accessed through the Europa server <http://europa.eu/>.

JRC 72196

EUR 25382 EN

ISBN 978-92-79-25312-6 (pdf)

ISBN 978-92-79-25313-3 (print)

ISSN 1831-9424 (online)

ISSN 1018-5593 (print)

doi:10.2788/32371

Luxembourg: Publications Office of the European Union, 2012

© European Union, 2012

Reproduction is authorised provided the source is acknowledged.

Printed in Italy

## TABLE OF CONTENTS

ACKNOWLEDGMENTS .....	4
1 INTRODUCTION.....	5
2 SCOPE AND OBJECTIVES OF THIS STUDY.....	6
3 EXPERIMENTAL .....	6
3.1 VEHICLE MATRIX.....	6
3.2 TEST FUELS AND LUBRICANTS .....	7
3.3 CYCLES AND TEST PROCEDURE.....	8
3.4 SAMPLING SYSTEMS AND CONDITIONS .....	10
3.4.1 PM SAMPLING .....	12
3.4.2 PARTICLE NUMBER SAMPLING .....	12
3.5 GASEOUS POLLUTANTS.....	14
4 RESULTS.....	15
4.1 Emissions over the regulated NEDC at 22°C.....	15
4.1.1 PM Emissions .....	15
4.1.2 Particle number emissions.....	15
4.2 Emissions over the CADC at 22°C .....	20
4.2.1 PM emissions.....	20
4.2.2 Particle number emissions.....	21
4.3 Effect of the test cell temperature .....	26
4.3.1 PFI vehicles .....	26
4.3.2 G-DI vehicles .....	28
4.4 Effect of fuel.....	32
4.4.1 Use of CNG on PFI2 .....	32
4.4.2 Use of E75/E85 on G-DI2 .....	35
4.5 GPF performance .....	38
4.6 G-DI/PFI emission performance .....	42
5 DISCUSSION & CONCLUSIONS .....	46

6 LIST OF SPECIAL TERMS AND ABBREVIATIONS.....49  
REFERENCES .....51

## **ACKNOWLEDGMENTS**

The authors would like to gratefully acknowledge the technical support of R. Colombo, M. Sculati, G. Lanappe, F. Muehlberger, and P. Le Lijour. The authors would like to especially acknowledge Dr. Christos Dardiotis for the fruitful discussions.

The study was partly funded by the EU FP7 project TRANSPHORM (Transport related air pollution and health impacts).

# 1 INTRODUCTION

Legislation limiting the pollutant emissions of new registered vehicles is well established in many regions of the world. One pollutant of special concern is Particulate Matter (PM), which is a complex physicochemical mixture of solid and volatile particles ranging in size from a few nanometers to up to around one micrometer in diameter. Historically, the PM emissions of automotive engines were regulated in terms of mass. Gasoline vehicles were not subjected to regulations due to their relatively low PM mass levels compared to their diesel counterparts.

However, the improvements in diesel technology brought by the progressively tighter emissions standards, raised concerns about the sensitivity of the gravimetric procedure to accurately quantify the true PM emission levels [1]. Furthermore, there is a growing consensus amongst the health experts that particles in the ultrafine range (smaller than 100 nm), which contribute little to the particulate mass due to their small size, are potentially more toxic and have greatest adverse health effects on human health [2]. These concerns about the limitations of the conventional gravimetric procedure led to the setting up of the Particle Measurement Programme (PMP) as a Working Group of the United Nations Economic Commission for Europe, Working Party on Pollution and Energy (UN-ECE GRPE).

The mandate given to the PMP Working Group by GRPE was to develop new particle measurement techniques to complement or replace the existing particulate mass measurement, with special consideration to measuring particle emissions at very low levels. PMP was also tasked with accumulating data on the performance of a range of engine/vehicle technologies when tested according to the proposed procedures. The PMP group concluded that a revised filter mass measurement method and a particle number method using a Condensation Particle Counter (CPC) and sample preconditioning to eliminate volatile particles, best met the objectives of the programme.

The proposed PMP methodology was subsequently evaluated in Light Duty and Heavy Duty Inter-Laboratory Correlation Exercises (ILCE\_LD, ILCE\_HD respectively). The ILCE\_LD was successfully completed [3] and the results of the ILCE\_LD report together with consultations with stakeholder groups including national Governments, the European Commission, the automotive industry, Tier 1 suppliers and the test houses were used to finalise a new Annex for the R83 which introduced the particle number procedure for certification testing. Modifications to the particulate mass measurement procedure were also integrated. The new procedures came into force with the official publication of the procedures during February 2009 [4].

Starting from September 2011 (Euro 5b stage), a limit value of 4.5 mg/km and  $6 \times 10^{11}$  #/km, following the PMP procedures, was introduced for the particulate mass and solid Particle Number (PN) emissions of all new registered diesel vehicles. Regulation (EC) No 715/2007 also authorized the Commission to introduce particle number emission limits for gasoline fueled vehicles. However, at the time of development of the implementing legislation it was decided that additional information is desirable on the emissions of these vehicles prior to a standard being set. In that respect, the introduction of a particle number limit was postponed at the Euro 6 stage (09/2014) the latest.

One of the major concerns regarding the regulation of particle number emissions from gasoline vehicle is the relevance and applicability of the PMP procedure to this category of vehicles. One issue pertains to the size of emitted particles since several studies suggested that these are smaller compared to those found in diesel exhaust and therefore the lower size

limit of 23 nm specified in the legislations might exclude a significant portion of the solid particle population. Another delicate issue is the availability of after-treatment technologies that might be required to control the particulate emissions of this vehicle category and perhaps more importantly the fuel penalty barrier associated with the introduction of these emission control technologies on the gasoline vehicle exhaust. This is particularly true in the case of direct injection gasoline vehicles whose particle number emission levels are currently about an order of magnitude above the diesel limit [3].

## **2 SCOPE AND OBJECTIVES OF THIS STUDY**

In December 2009 Directorate General (DG) Enterprise (ENTR) and the Joint Research Centre (JRC) signed an Administrative Arrangement to fix the terms of a project titled “Scientific/technical support to the preparation and implementation of light-duty vehicle emission legislation”.

The Commission Regulation (EC) No 692/2008 of 18 July 2008 [5] together with the Regulation (EC) No 715/2007 of the European Parliament and of the Council of 20 June 2007 [6] set the regulatory framework for type-approval of motor vehicles with respect to emissions from light passenger and commercial vehicles (Euro 5 and Euro 6). In particular these regulations set the emission standards and the related implementing measures, divided into three different steps, that will enter into force between 2009 (Euro 5) and 2014 (Euro 6). However, the above mentioned Regulations leave open some issues regarding the Euro 5b and the Euro 6 emissions standards to be addressed and defined before the entry into force of these pieces of legislation [7]. The services requested by the DG ENTR to JRC were detailed in a series of deliverables, among which this report.

At a first step, the JRC investigated the particle number emission performance of gasoline vehicles by compiling information found in the literature as well as experimental data collected at the Vehicle Emission Laboratory (VELA) [8]. The objective of this follow-up study is twofold:

- To assess the particle number measurement procedure, currently applicable to diesel vehicles, for their gasoline counterparts, mainly with respect to the lowest detectable particle size.
- To experimentally assess the performance of various emission reduction options for gasoline fuelled vehicles, including the use of particulate filters, cleaner fuels and improved combustion concepts.

## **3 EXPERIMENTAL**

### **3.1 VEHICLE MATRIX**

Five in total gasoline vehicles were tested in this study. Two of them were equipped with a Port Fuel Injection (PFI) system, two employed direct injection into the cylinder (G-DI) and one was equipped with a twin injection system allowing fuel injection both in the intake port and inside the cylinder (G-DI/PFI). All gasoline vehicles tested, run stoichiometrically. Two late technology diesels equipped with a Diesel Particulate Filter (DPF) were also tested to serve as a reference. The main characteristics of the vehicles tested are summarized in Table 1.

One of the G-DI vehicles (G-DI1) was retrofitted in some tests with a prototype Gasoline Particulate Filter (GPF) made of acicular mullite, specifically designed for application on this vehicle model. The GPF was installed 90 cm downstream of the single, close-coupled Three Way Catalyst (TWC) of the vehicle using a specially designed canning. A dummy, hollow canning of the same dimensions, installed in place of the GPF, provided the means to establish the baseline emission levels of the vehicle.

The second G-DI tested (G-DI2) was a Euro 5 certified Flexi Fuel Vehicle (FFV) capable of running on ethanol fuel blend of up to 85% by volume ethanol. One of the PFIs tested (PFI2) was a Euro 4 certified Bi-Fuel vehicle running on gasoline, and CNG/H<sub>2</sub> mixtures. The other PFI vehicle (PFI1) was Euro 5 certified and incorporated a start-stop system which however was deactivated during the measurements. The same vehicle was tested in the past at the JRC with this feature activated (vehicle PFI\_E5\_1 in [8]) and therefore a direct comparison of the results allows for a quantification of its effect on the vehicle particulate emissions.

One of the DPF equipped diesels (DPF1) was Euro 5 certified and incorporated a DPF downstream of an oxidation catalyst both being close-coupled to the engine. The particulate emission performance of this vehicle is described in more details elsewhere [9]. The second DPF (DPF2) was Euro 6 compliant and incorporated in addition to a DPF a Selective Catalytic Reduction (SCR) system.

Table 1: Vehicle data and specifications.

Vehicle Code	Emission Standard	Fuel System	Engine	Mileage [km]
G-DI1	Euro 5	G-DI	1984 cc, 132 kW	12461
G-DI2	Euro 5	G-DI FFV	1984 cc, 132 kW	1441
G-DI/PFI	Euro 4	G-DI/PFI	4608 cc, 280 kW	28641
PFI1	Euro 5	PFI	1368 cc, 57 kW	42146
PFI2	Euro 4	PFI Bi-Fuel	1242 cc, 44 kW	2343
DPF1	Euro 5	Common rail	1248 cc, 55 kW	6402
DPF2	Euro 6	Common rail	1968 cc, 105 kW	22284

### 3.2 TEST FUELS AND LUBRICANTS

The gasoline vehicles were tested on petrol fuel containing no ethanol (E0) with the exception of the G-DI2 FFV vehicle. The latter was tested on ethanol/gasoline blends of 5% (E5), 75% (E75) and 85% (E85) on a volumetric basis. The two diesel vehicles were tested on commercial diesel fuel. The Bi-Fuel vehicle (PFI2) was also tested on a range of Compressed Natural Gas (CNG) and Hydrogen (H<sub>2</sub>) mixtures, spanning from 100% CNG to 70% CNG and 30% H<sub>2</sub>. Two different CNG fuels were employed differing in the CH<sub>4</sub> content

(86% (G25) and 100% (G20)). All fuels complied with the specifications laid down in Directive 2009/30/EC [10].

All vehicles were tested with the lubricant contained upon receipt from the different suppliers.

### 3.3 CYCLES AND TEST PROCEDURE

All vehicles were tested under the standard New European Driving Cycle (NEDC) shown in Figure 1. The cycle has been used in Europe for certification of light-duty vehicles since 2000 and consists of the urban part, commonly indicated as ECE, which includes four repetitions of the ECE15 elementary cycle, and the extra-urban part (EUDC), while it is performed with the engine cold (at least 6 hours soak).

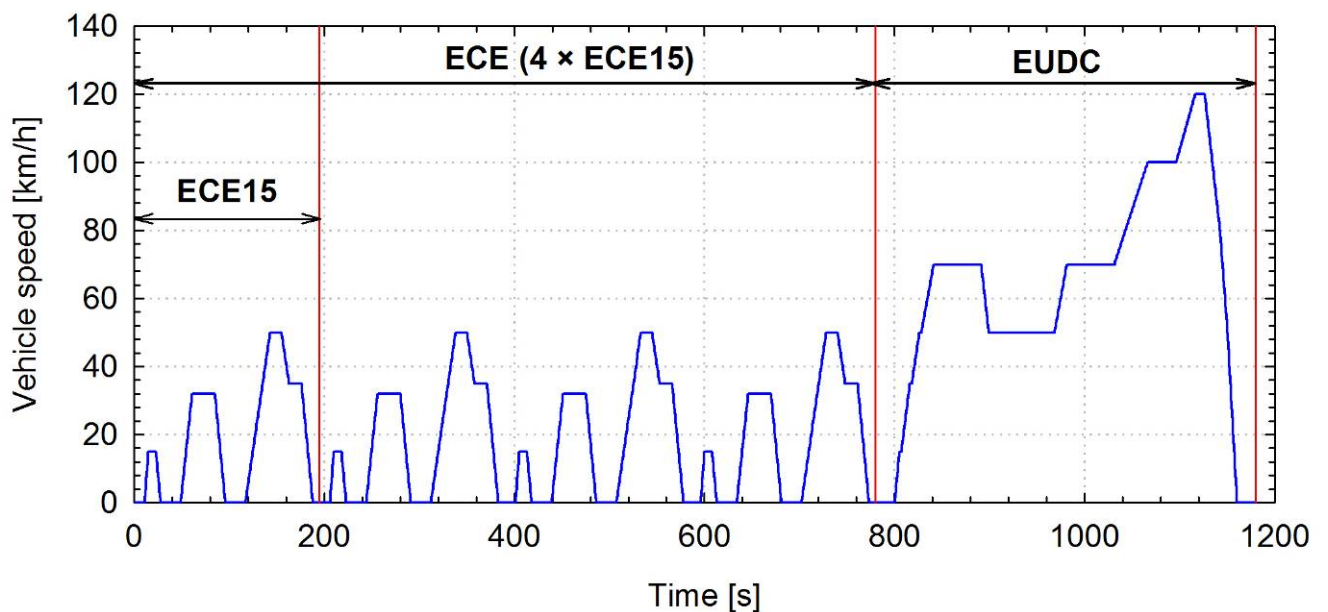


Figure 1: New European Driving Cycle (NEDC) and its two phases: Urban (ECE) and Extra-Urban (EUDC).

The G-DI and DPF vehicles were also tested over a real world driving cycle developed in the framework of the ARTEMIS project [11], the speed profile of which is shown in Figure 2. This cycle, named Common Artemis Driving Cycle (CADC) by convention, was developed by statistical analysis of speed profile databases of 90000 km accumulated from on-board monitoring of 80 passenger cars in France, Germany, Great Britain and Greece, supplemented by another 10000 km collected in Switzerland and Italy under controlled traffic conditions. It has a total duration of 40 minutes and consists of three main phases representative of urban, rural and motorway driving conditions in Europe, with some conditioning phases in-between.

The G-DI1 vehicle was also tested at 50, 90 and 120 km/h steady speed cruising under road load, with the engine running hot. These dedicated tests were performed in order to enable measurement of the number-weighted size distributions of the emitted exhaust aerosol with a Scanning Mobility Particle Sizer (Section 3.4.2).

The G-DI vehicles were measured at both 22°C and -7°C test cell temperatures. For the sub-zero temperature tests the dynamometer settings are adjusted for a 10% decrease of the coast-down time (resulting in a corresponding increase of the resistance to progress) in accordance to the UN Regulation 83 proposal for 06 series of amendments [12]. The G-DI2

vehicle when running on E5 was additionally tested at 15°C over the NEDC, in which case the dynamometer settings were the same to those at 22°C.

The two PFI vehicles were only measured over the NEDC cycle. Tests were performed at 15°C, 22°C and 25°C. Figure 3 illustrates the protocol followed in the testing while Table 2 summarizes the number of tests performed at each cycle, temperature and fuel combination.

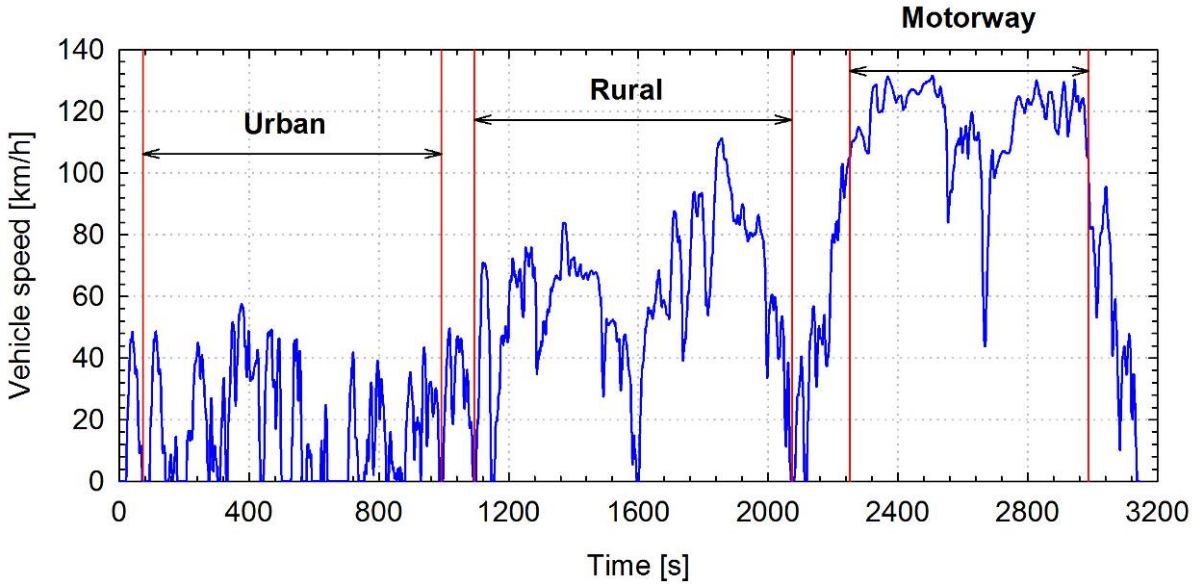


Figure 2: Common Artemis Driving Cycle and the three sampling phases representative of urban, rural and motorway driving.

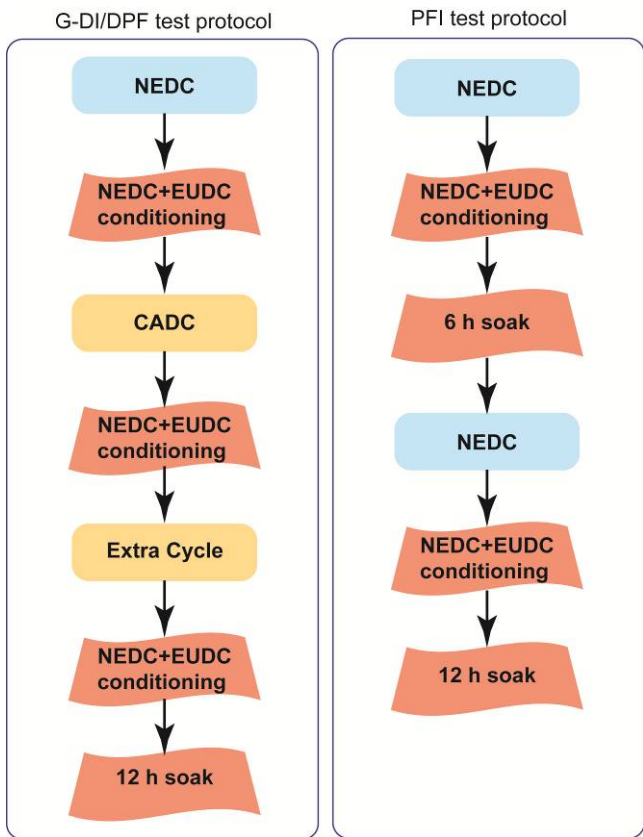


Figure 3: Daily test sequence employed for the tests of G-DI and DPF vehicles (left-hand panel) and the PFI vehicles (right-hand panel)

Table 2: Combinations of vehicle, cycle, fuel and test cell temperatures tested.

Vehicle	Fuel	NEDC				CADC	
		-7°C	15°C	22°C	25°C	-7°C	22°C
G-DI1	E0	2		3			3
GPF	E0			3			
G-DI2	E5	3	3	5		2	4
G-DI2	E75/E85	3		3		2	3
G-DI/PFI	E0	2		2		2	2
PFI1	E0		2	2	2		
PFI2	E0		2	2	2		
PFI2	CNG			2, 2*			
PFI2	95%CNG - 5%H <sub>2</sub>			2, 2*			
PFI2	90%CNG - 10%H <sub>2</sub>			2, 2*			
PFI2	85%CNG - 15%H <sub>2</sub>			2, 2*			
PFI2	80%CNG - 20%H <sub>2</sub>			2, 2*			
PFI2	75%CNG - 25%H <sub>2</sub>			2, 2*			
PFI2	70%CNG - 30%H <sub>2</sub>			2, 2*			
DPF1	diesel	4		6		2	5
DPF2	diesel	4		5		3	4

\* 2 repetitions with G20 CNG and 2 with G25 CNG

### 3.4 SAMPLING SYSTEMS AND CONDITIONS

The tests were carried out on a 48" 4×4 dynamometer MAHA SN 87 (roller diameter of 48 in and 150 kW) at the JRC Vehicle Emissions Laboratory (VELA).

Sampling was conducted according to the current legislation. The exhaust gas was primarily diluted and conditioned following the Constant Volume Sampling (CVS) procedure. The CVS tunnel was equipped with high efficiency filters for particles and hydrocarbons that reduce particle contributions from the dilution air to near zero levels (99.99% reduction of particles with size diameter of 0.3  $\mu\text{m}$ ). The temperature of the dilution air was conditioned to  $23\pm 1^\circ\text{C}$  during all tests.

The vehicles were coupled to the CVS transfer line by a metal-to-metal joint during testing to avoid the possibility of exhaust contamination by the high-temperature breakdown of elastomer coupling elements. The exhaust was transported to the tunnel through a 5.5 m long insulated corrugated stainless steel tube. It was introduced along the tunnel axis, near an orifice plate that ensured rapid mixing with the dilution air. The flow rate of diluted exhaust gas through the tunnel was controlled by a critical orifice venturi. A flowrate of 6, 8 or 9  $\text{m}^3/\text{min}$  at standard reference conditions (20  $^\circ\text{C}$  and 1 bar), was employed depending on the vehicle size and driving cycle. The exact flowrates employed in the campaign are summarized in Table 3.

A schematic of the sampling set up employed for particulate characterization is illustrated in Figure 4. In general four different probes, placed at the same cross-section of the tunnel and facing upstream the flow, were used for sampling. Two probes were employed for particle number characterization and one other for filter collection. These probes were installed 10 tunnel diameters downstream of the mixing point to ensure complete mixing of the dilution air and the exhaust gas.

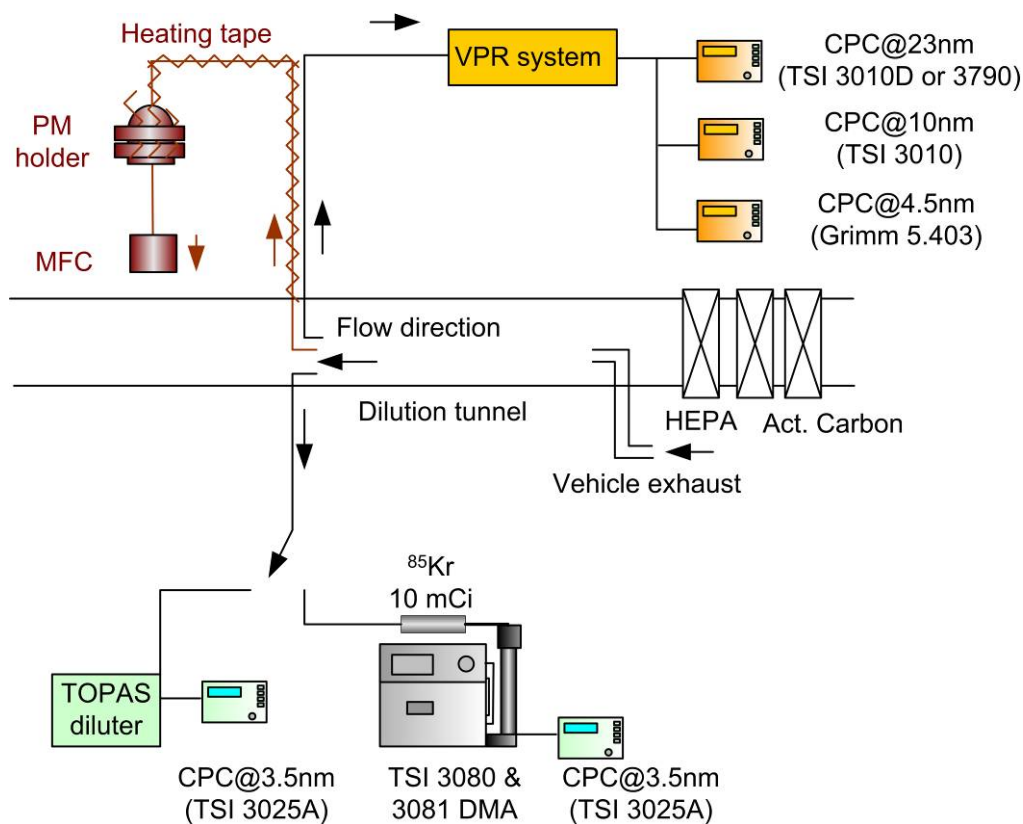


Figure 4: Experimental set up.

Table 3: CVS flowrates (m<sup>3</sup>/min) employed for each vehicles and fuel combination.

Vehicle	NEDC	CADC
G-DI1	6	9
G-DI2	8	8
G-DI/PFI	9	9
PFI1	6	-
PFI2	6	-
DPF1	6	8
DPF2	6	8

### 3.4.1 PM SAMPLING

PM Samples were drawn directly from the CVS at a constant flowrate of 50 lpm at normal conditions (0 °C and 1 bar). The filter holder and transfer tubing were externally heated by direct surface heating to permit aerosol stabilization of >0.2 s prior to sampling and to ensure close control of the filter face temperature to 47 °C (±5 °C). A single 47 mm Teflon-coated glass-fiber Pallflex® TX40H120-WW was employed for the entire NEDC and another one for all three sampling phases of the CADC.

The filters were kept in a control temperature and humidity chamber (22±1 °C and 50±5% respectively), and they were weighted with a Mettler Toledo model UMX2 balance (sensitivity 10<sup>-7</sup> g) before and after the measurement, allowing at least two hours for conditioning. Electrostatic charge effects were minimized by the use of HAUG Type EN SL LC 017782100 neutralizer and grounded conductive surfaces. Each filter was weighted two times, and the average of the weightings was used in calculating mass changes.

### 3.4.2 PARTICLE NUMBER SAMPLING

Aerosol samples for particle number measurement were drawn from the CVS tunnel through two different probes. One branch was used to characterize thermally treated particles while the other branch was used to monitor the number concentration of the total particle population inside the CVS tunnel.

Thermal treatment was performed in accordance to the PMP methodology. Samples taken from the CVS tunnel were diluted at a first stage using condition air at 150°C. The diluted sample was subsequently heated in an evaporating tube maintained at a wall temperature of 350°C and then immediately diluted using conditioned air at ambient temperature. Two different PMP compliant systems were employed in the study. One was developed by Matter Aerosol AG [13, 14, 15] while the second one is commercialized by AVL GmbH (APC) [16]. The concentration of the thermally treated sample was then monitored with three CPCs, having nominal 50% counting efficiencies ( $d_{50}$ ) of 23 nm (TSI 3790 or TSI 3010D), 10 nm (TSI 3010) and 4.5 nm (Grimm 5403), respectively. In the G-DI1 vehicle tests, the TSI 3010 CPC operated at an elevated temperature difference of 23°C that effectively shifted  $d_{50}$  to 6.5 nm.

One concern regarding the application of the PMP methodology to measurements of sub-23 nm particles, pertains to the possibility of volatile artifact interference due to (re-)nucleation of vapours (especially sulfates [17]) downstream of the evaporating tube. Since the nucleation rate is a highly non-linear function of the vapour concentration, it is expected that increased dilution ratios at the primary stage would suppress volatile particle formation. In order to investigate whether such nucleation mode volatile particles contributed to the measured particle counts, tests were performed at different primary dilution ratios.

The total number concentration of particles inside the CVS tunnel was monitored with a TSI 3025A CPC (nominal 50% counting efficiency at 3.5 nm) running at high flow (1.5 lpm). A TOPAS DDS560 diluter (dilution bridge) was employed upstream of the 3025A CPC to bring the concentrations within the operating range of the CPC. In some limited tests of the G-DI1 vehicle, the 3025A CPC was connected to a TSI 3936L25 Scanning Mobility Particle Sizer (SMPS) to monitor the number weighted mobility size distributions over steady speed cruising at 50, 90 and 120 km/h.

In total three different PMP compliant CPCs (nominal  $d_{50}$  at 23 nm) were employed in the study. Two of them were TSI 3790 models originally supplied with the two PMP systems used in the study, while the other one was a TSI 3010D model which was employed in all DPF1 and DPF2 tests. The 3025A CPC was calibrated against an electrometer in dedicated tests presented elsewhere [18]. The slopes of the other CPCs employed in the study were compared to that of the calibrated 3025A CPC on several occasions during the measurement campaign, using monodisperse particles of 100 nm produced in a Tandem Differential Mobility Analyzer setup described in [18]. Table 4 summarizes the calculated slopes that were employed in the calculations.

Table 4: Measured slopes of the different CPCs employed in the study

CPC	3025A	Grimm	3010	3790_1	3790_2	3010D
Slope	1.00	0.97	0.82	0.90	0.90	0.88

Table 5 summarizes the PMP system (Volatile Particle Remover and CPC at 23 nm) as well as the Particle Concentration Reduction Factors (PCRFs) employed in the testing of the different vehicles.

Table 5: VPR settings employed at the tests of the different vehicles

Vehicle	PMP system	PCRFs	PMP CPC
G-DI1	AVL APC	1000 (100×10), 2000 (200×10)	TSI 3790_1
G-DI1 & GPF	AVL APC	100 (10×10), 1000 (100×10)	TSI 3790_1
G-DI2	Matter Aerosol	2000 (200×10), 3500 (350×10)	TSI 3790_2
G-DI/PFI	Matter Aerosol	1750 (350×5), 500 (100×5), 250 (50×5)	TSI 3790_2
PFI1	Matter Aerosol	2000 (200×10)	TSI_3790_2
PFI2	AVL APC	250 (25×10), 1000 (100×10)	TSI 3790_1
DPF1	Matter Aerosol	300 (30×10), 500 (50×10), 2000 (200×10)	TSI 3010D
DPF2	AVL APC	250 (25×10), 500 (50×10), 2000 (200×10)	TSI 3010D

### 3.5 GASEOUS POLLUTANTS

A Horiba MEXA-7400HTR-LE analyzer was employed for the real time measurement of the gaseous pollutants (Nitrogen Oxides - NO<sub>x</sub>, Total Hydrocarbons – THC, Carbon Monoxide - CO and dioxide - CO<sub>2</sub>) and Oxygen (O<sub>2</sub>). The Horiba MEXA-7400HTR-LE analyzer was also employed to measure bag emissions in accordance to the current UN Regulation 83 [19]. The real time traces of O<sub>2</sub>, CO<sub>2</sub>, CO and HC provided the means for the calculation of lambda, according to the same regulation [19].

## 4 RESULTS

### 4.1 Emissions over the regulated NEDC at 22°C

#### 4.1.1 PM Emissions

Figure 5 summarizes the PM emissions of all vehicles tested over the NEDC. All vehicles complied with the Euro 5 limit of 4.5 mg/km applicable to diesels and G-DIs. G-DI vehicles stand out exhibiting higher PM emissions from both PFIs and DPFs. Yet the highest emitting G-DI vehicle (G-DI/PFI hybrid) emitted on average 2.0 mg/km ( $\pm 0.11$  mg/km)<sup>1</sup>, that is less than half the applicable limit. The PM emissions of the other two G-DI vehicles averaged at 1.3 mg/km ( $\pm 0.11$  mg/km) and 0.7 mg/km ( $\pm 0.11$  mg/km). The installation of a GPF on G-DI1 and the use of E85 fuel in G-DI2 effectively reduced the PM emissions at the levels of DPF and PFI vehicles (approximately 0.4 mg/km).

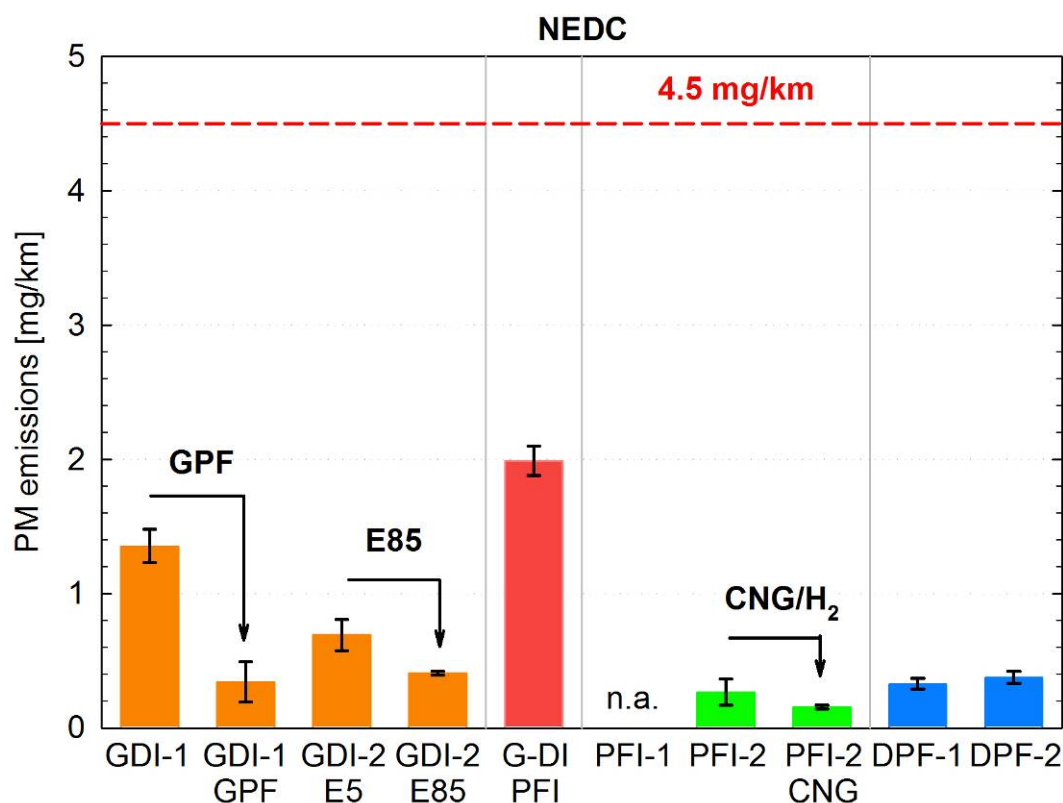


Figure 5: PM emissions of the different vehicles tested over the NEDC. Error bars stand for  $\pm$  one standard error.

#### 4.1.2 Particle number emissions

Figure 6 summarizes the average particle number emissions of the different vehicles over the NEDC at 22°C as determined with the different CPCs. The figure also shows the relative

<sup>1</sup> The range shown in parenthesis next to the average emission levels corresponds to  $\pm 1$  standard error, determined as the standard deviation divided by the square root of the number of repetitions.

fractions of thermally treated exhaust measured with the CPCs having a  $d_{50}$  below 23 nm that were not detected by the PMP compliant CPC ( $d_{50}$  at 23 nm, hereinafter CPC\_PMP).

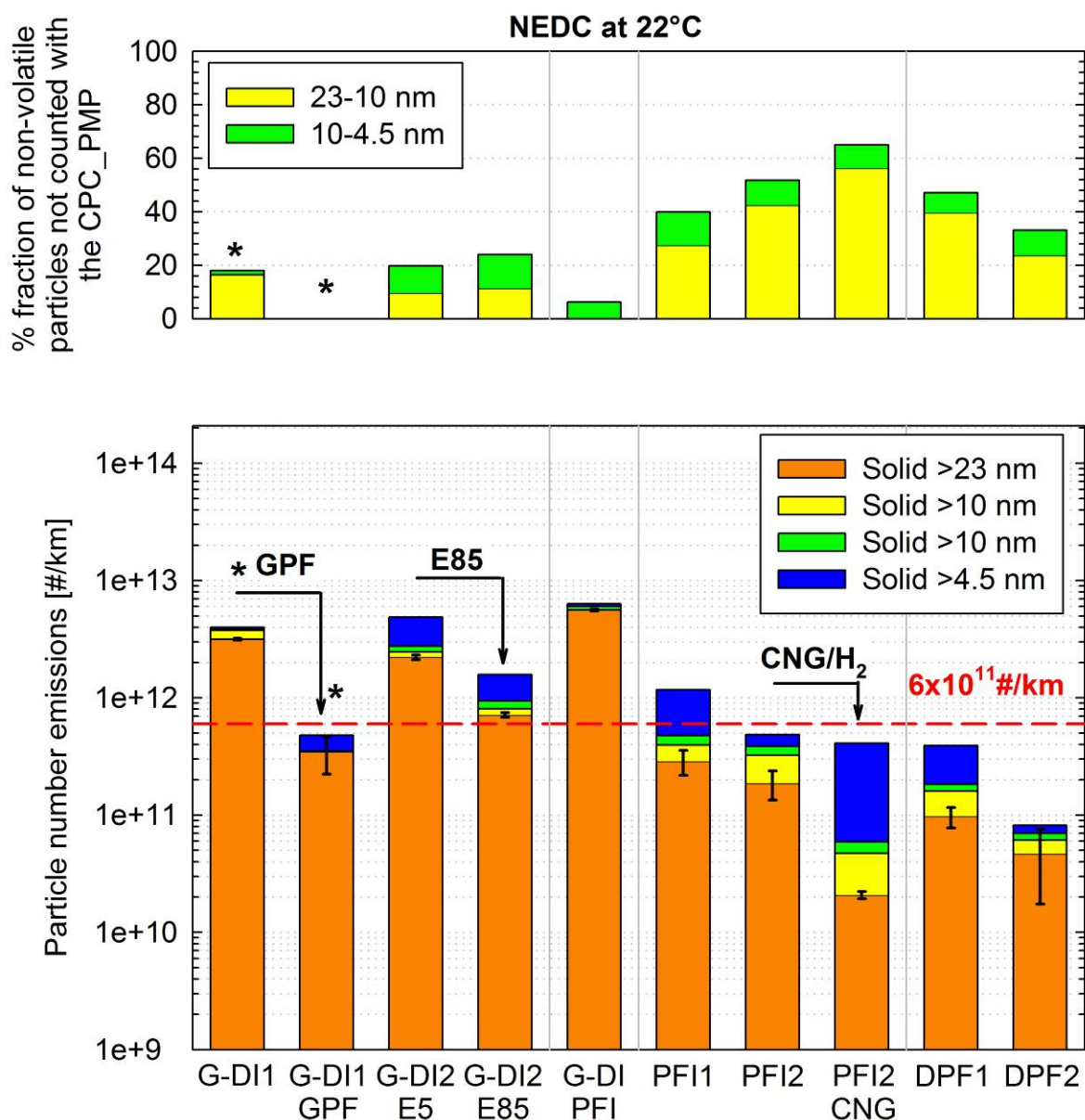


Figure 6: Particle number emission rates of the different vehicles tested over the NEDC (bottom panel) and fraction of sub-23nm non-volatile particle counts not detected with the PMP CPC (top panel). In the bottom panel, orange bars correspond to number emission rates of non-volatile particles determined with the CPC having a  $d_{50}$  at 23 nm, yellow bars show the excess emissions measured downstream of the VPR with the CPC having a  $d_{50}$  at 10 nm (\* or 6.5 nm in the case of G-DI1), green bars indicate the excess emissions measured downstream of the VPR with the CPC having a  $d_{50}$  at 4.5 nm, while blue bars show the excess emissions of thermally untreated samples measured with the CPC having a  $d_{50}$  at 3.5 nm. Error bars stand for  $\pm$  one standard error of the measured number concentrations according to the regulatory procedure ( $d_{50}$  at 23 nm). In the top panel, yellow bars indicate the fraction of particle concentrations measured with the CPC at 10 nm not counted by the CPC at 23 nm, while green bars correspond to the excess fraction of particle concentrations measured with the CPC at 4.5 nm not detected by the CPC at 23 nm.

Focusing at the particle number emissions determined in accordance to the PMP methodology, it can be seen that all three G-DI vehicles when tested on gasoline or 5% ethanol, emitted systematically above the diesel limit of  $6 \times 10^{11} \text{ #/km}$ . On average, the emissions were  $3.2 \times 10^{12} \text{ #/km}$  ( $\pm 5.2 \times 10^{10} \text{ #/km}$ ),  $2.2 \times 10^{12} \text{ #/km}$  ( $\pm 1.1 \times 10^{11} \text{ #/km}$ ) and

$5.6 \times 10^{12}$  #/km ( $\pm 1.2 \times 10^{11}$  #/km) for the G-DI1, the G-DI2 running on E5 and the G-DI/PFI, respectively. The installation of the GPF on G-DI1, effectively reduced the particle number emissions by approximately one order of magnitude, averaging at  $3.5 \times 10^{11}$  #/km ( $\pm 1.2 \times 10^{11}$  #/km). A significant ( $\sim 70\%$ ) reduction was also observed in the G-DI2 vehicle when running on E85, with the emissions averaging at  $7.1 \times 10^{11}$  #/km ( $\pm 3.7 \times 10^{10}$  #/km). The beneficial effect of ethanol (at such high proportions) on the particle number emissions of G-DI vehicles was also reported elsewhere [20, 21].

The two PFI vehicles emitted systematically below  $6 \times 10^{11}$  #/km. The emissions of PFI1 vehicle averaged at  $2.9 \times 10^{11}$  #/km ( $\pm 7.3 \times 10^{10}$  #/km). The same vehicle tested with the start-stop feature activated was found to emit  $5.5 \times 10^{11}$  #/km ( $\pm 2.9 \times 10^{10}$  #/km) (PFI\_E5\_1 in [8]), that is 90% higher. An examination of the real time traces (Figure 7) suggests that the main difference mainly originates from elevated emissions over the second ECE15 segment of the cycle. This is indicative of prolonged warming up period due to the engine being switched off at idling.

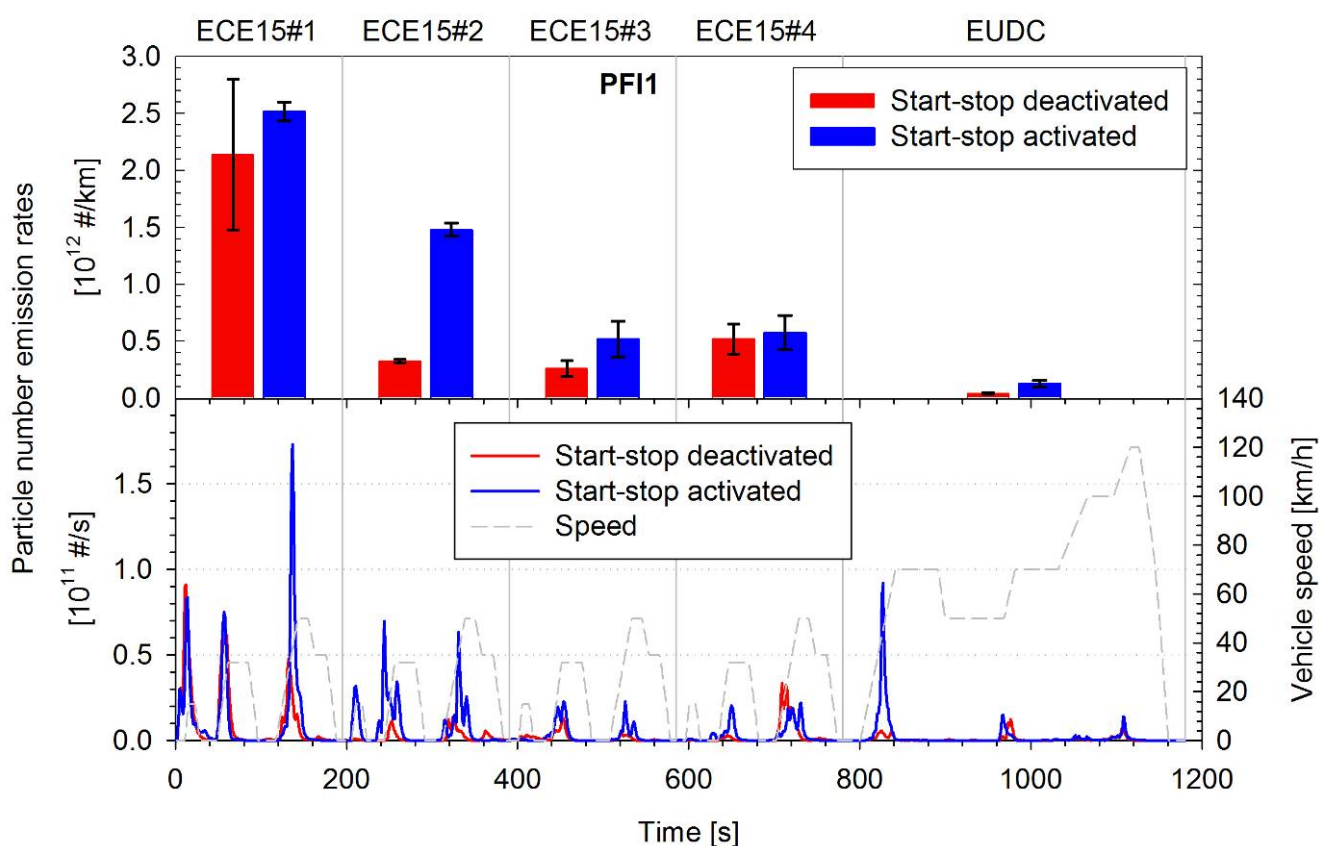


Figure 7: Real time particle number emission rates in #/s of the PFI1 over the NEDC (bottom panel) and average emission rates in #/km over the 4 ECE15 and the EUDC segments of the cycle (top panel), when the start stop feature was activated (red bars and lines) and deactivated (blue bars and lines). Error bars stand for  $\pm$  one standard deviation.

When the Bi-fuel vehicle (PFI2) operated on CNG/H<sub>2</sub> mixtures, the regulated particle number emissions were reduced by one order of magnitude. The emission performance of this vehicle when running on CNG/H<sub>2</sub> is addressed in more details in section 4.4.1.

The regulated particle number emissions of the two DPF equipped diesels over the NEDC were well below the diesel PN limit. DPF1 emitted on average  $9.7 \times 10^{10}$  #/km

( $\pm 2.0 \times 10^{10}$  #/km) and while the emissions of the DPF2 vehicle averaged at  $4.7 \times 10^{10}$  #/km ( $\pm 1.2 \times 10^{10}$  #/km). The relatively large variability (the Coefficient of Variation being 50% and 137% respectively) is to a large extent associated with changes of the fill status of the DPF that directly affect the filtration efficiency (as shown for the case of DPF1 in [9]).

The top panel of Figure 1 shows the relative fraction of particles measured downstream of the VPR with the two CPCs having a  $d_{50}$  below 23 nm that were not actually detected by the PMP compliant CPC. In the tests with the FFV G-DI vehicle, the CPC\_PMP did not detect 10% of the particles measured with the CPC having a  $d_{50}$  at 10 nm (hereinafter CPC@10) and ~20% of the particles counted by the CPC with a  $d_{50}$  at 4.5 nm (hereinafter CPC@4.5), irrespective of the fuel employed (E5 or E85). Similar trends were observed in the other G-DI vehicle tested at its OEM configuration (G-DI1), with the CPC\_PMP not detecting 18% of the particles counted by the CPC@4.5. In these particular tests, the TSI 3010 CPC operated at a  $d_{50}$  of 6.5 nm (by means of changing the operating temperatures) and measured almost the same concentrations with the CPC@4.5.

A higher fraction of smaller particles were detected in all PFI vehicle tests. More specifically, the CPC\_PMP did not detect 27% (PFI1) to 42% (PFI2) of the particles measured with the CPC@10 for the tests on gasoline. A relatively higher uncounted fraction (56% on average) was observed when the PFI2 was tested on CNG/H<sub>2</sub> mixtures. The excess particle counts detected by the CPC@4.5 were approximately 10% higher for both gasoline and CNG.

When the GPF was installed on G-DI1 vehicle, the three CPCs sampling downstream of the VPR measured practically the same concentrations. This suggests that the particular GPF was actually more efficient in retaining smaller particle sizes. Interestingly though, both DPF equipped diesels appeared to have emitted relatively high quantities of nano-sized non-volatile particles. The CPC\_PMP did not detect 39% (DPF1) and 23% (DPF2) of the particles counted by the CPC@10. The corresponding fractions of the excess particles counted by the CPC@4.5 were 47 and 33%, respectively.

In interpreting the observed differences in the indications of the different CPCs, it is important to realize that the CPC\_PMP does not have a sharp cut-off size at 23 nm. Furthermore, the two PMP CPC employed in the present study are calibrated by the manufacturer on emery oil. Yet, both CPC models were found to be less efficient in detecting soot [22, 23] and graphite [18] particles. Effectively, the counting efficiency for soot aerosol is shifted towards larger sizes but there are also indications that the slope of the CPC deteriorates [18]. The latter is not expected to have affected the results in this study as the slope of the CPCs was determined against graphite particles (Table 4). Experimentally determined counting efficiencies of the TSI 3790\_1 CPC against graphite particles (shown in the left-hand panel of Figure 8) suggest that the  $d_{50}$  value is actually 26.5 nm and that 20% of 41 nm particles will not be counted.

The material dependence of the counting efficiencies was found to decrease when increasing saturation ratios inside the CPC condenser (that is as the operating  $d_{50}$  point is shifted towards smaller sizes), in line with what the heterogeneous nucleation theory predicts [24]. Therefore it is not expected to be that evident in the CPCs with a lower cut-off size, which furthermore exhibit a steeper efficiency curve (as evident in the nominal counting efficiency curves of the CPC@10 and the CPC@4.5 shown also in Figure 8).

Overall, the fraction of nano-sized particles not being detected by a CPC\_PMP is expected to depend on the underlying size distribution. In order to investigate the nature of this dependence, some numerical simulations were performed using a range of lognormal

distributions. The results of these simulations are shown on the right-hand panels of Figure 8. The calculations suggest that the fraction of nano-sized particle not detected by the CPC\_PMP practically depends only on the geometric mean diameter ( $d_g$ ), ranging from less than 3% at  $d_g=100$  nm to up to 69% at  $d_g=20$  nm. The estimated excess particles counted by the CPC@4.5 compared to those measured with the CPC@10 increases with decreasing the peak diameter and with increasing the width of the distribution. Yet, the maximum excess contribution is less than 7%, occurring for a peak at 20 nm.

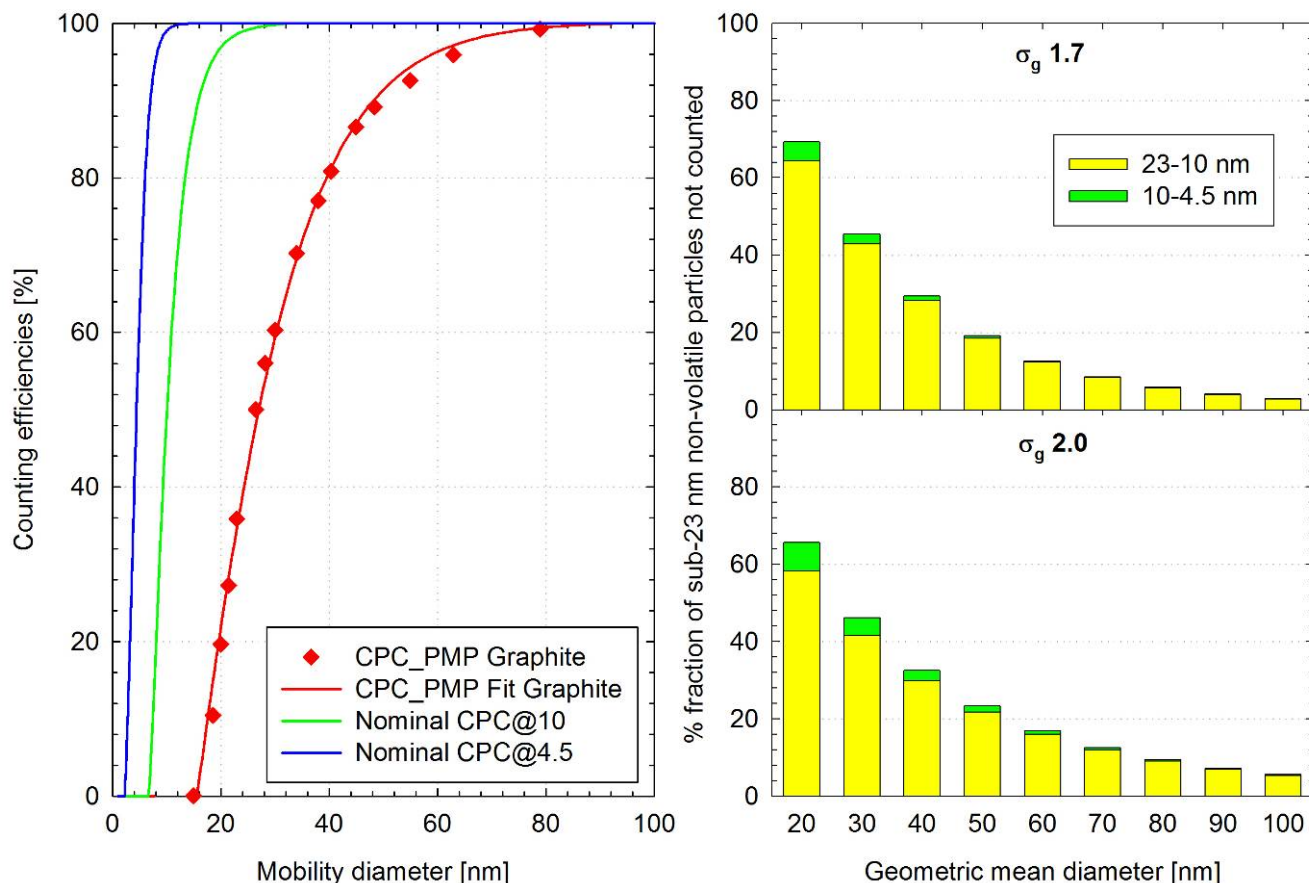


Figure 8: Counting efficiency curves (left-hand panel) of the CPC\_PMP (red curve), the CPC@10 (green curve) and the CPC@4.5 (blue curve) and calculated fractions of particle numbers not counted by the CPC\_PMP compared to the CPC@10 (yellow bars) and CPC@4.5 (green bars) as a function of the geometric mean diameter (horizontal axis) for lognormal distributions with geometric standard deviation of 1.7 (top-right panel) and 2.0 (bottom-right panel).

The results of these simulations assist in the interpretation of the experimentally observed CPC differences presented in the top panel of Figure 6. Focusing on the excess counts detected by the CPC@4.5 nm, the G-DI results are characteristic of a lognormal distribution peaking at 45-55 nm (G-DI2) to 52-58 nm (G-DI1), depending on the geometric standard deviation assumed, when gasoline PFI results are indicative of lognormal distributions peaking in the 27 nm (PFI2) to 35 nm (PFI1) range. The use of CNG on PFI2 resulted in a shift to even lower sizes, representative of a lognormal distribution peaking at ~20 nm. The results for the two DPF equipped diesels were representative of lognormal distributions peaking at 30 nm (DPF1) and 40 nm (DPF2).

It should be stressed at this point that these estimated peak diameters were based on the assumption of lognormal distributions. Published data on the size distributions of G-DI [25,

26] and PFI [25, 27] vehicles suggest a skewness towards small sizes and even the presence of a distinct solid nucleation mode [28, 29]. Such deviations from log-normality will effectively result in an underestimation of the true peak distribution size when using the CPC traces.

The relative differences between the CPC@4.5 and the CPC@10 were somehow higher from what the simulations on lognormal distributions would suggest (1-7%) but generally low (8-12%). This suggests that a formation of a distinct nucleation mode artifact below 10 nm like that observed by Swanson and Kittelson [30] is highly unlikely or if present should be small in magnitude, at least over the NEDC. Such small deviations may rather originate from uncertainties in the employed CPC slopes or even deviations of the distributions from log-normality.

## **4.2 Emissions over the CADC at 22°C**

### **4.2.1 PM emissions**

Figure 9 summarizes the PM emissions of the different vehicles tested over the CADC at 22°C. The conventional G-DI vehicles were found to emit elevated PM levels over the CADC compared to the NEDC tests (Figure 5). PM emissions of G-DI1 averaged at 1.96 mg/km ( $\pm 0.04$  mg/km) while those of G-DI2 running on E5 averaged at 2.64 mg/km ( $\pm 0.55$  mg/km). The use of E85 fuel was again beneficial and similar in magnitude to that observed over the NEDC (34% over CADC compared to 41% over NEDC). The introduction of the GPF was again proven to be very efficient, reducing the PM emissions to 0.31 mg/km ( $\pm 0.55$  mg/km), which corresponds to an 85% reduction over the baseline (the corresponding figure over the NEDC was 75%). Similar levels of PM were measured with DPF1 (0.33 mg/km  $\pm 0.01$  mg/km), while DPF2 was found to emit almost 3 times this figure (0.85 mg/km  $\pm 0.02$  mg/km). Such an increase over the NEDC could not be verified by the particle number measurements (section 4.2.2) and therefore reflects elevated emissions of volatile compounds. The PM emissions of the G-DI/PFI vehicle were significantly lower over the CADC averaging at 0.30 mg/km ( $\pm 0.55$  mg/km), i.e. 85% lower compared to the NEDC. As will be shown later (Section 4.6) this different emission behaviour is mainly associated with the cold start excess emissions.

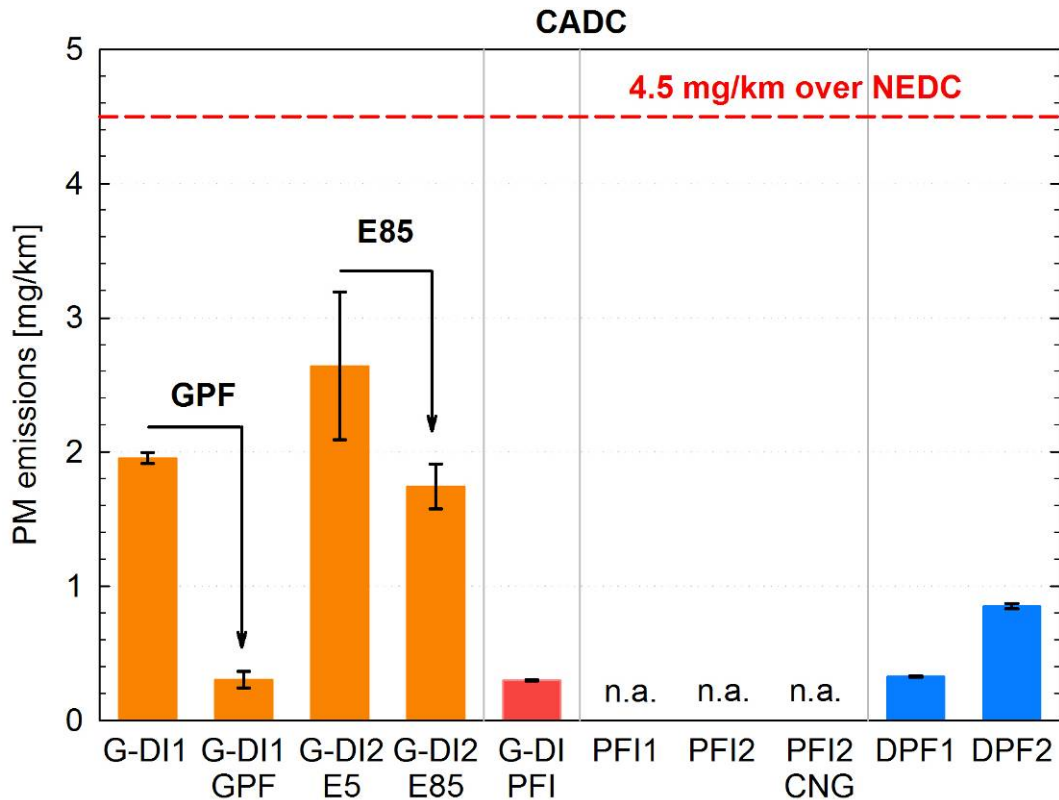


Figure 9: PM emissions of the different vehicles tested over the CADC. Error bars stand for  $\pm$  one standard error.

#### 4.2.2 Particle number emissions

The particle number emissions of the vehicles tested over the CADC test cycle are summarized in Figure 10, Figure 11 and Figure 12 for the urban, rural and motorway phases, respectively.

Focusing at the particle numbers following the regulated procedure, it can be seen that the emissions of the conventional G-DI vehicles running on gasoline, remained at levels above  $6 \times 10^{11}$  #/km for all phases of the CADC. G-DI1 emitted on average  $5.6 \times 10^{12}$  #/km ( $\pm 3.7 \times 10^{11}$  #/km) over the urban part,  $3.8 \times 10^{12}$  #/km ( $\pm 2.1 \times 10^{11}$  #/km) over the rural phase and  $2.4 \times 10^{12}$  #/km ( $\pm 0.8 \times 10^{11}$  #/km) over CADC motorway. The corresponding figures for the G-DI2 running on E5 were  $4.7 \times 10^{12}$  #/km ( $\pm 5.1 \times 10^{11}$  #/km),  $1.8 \times 10^{12}$  #/km ( $\pm 3.2 \times 10^{11}$  #/km) and  $1.8 \times 10^{12}$  #/km ( $\pm 2.6 \times 10^{11}$  #/km) over the urban, rural and motorway phases, respectively.

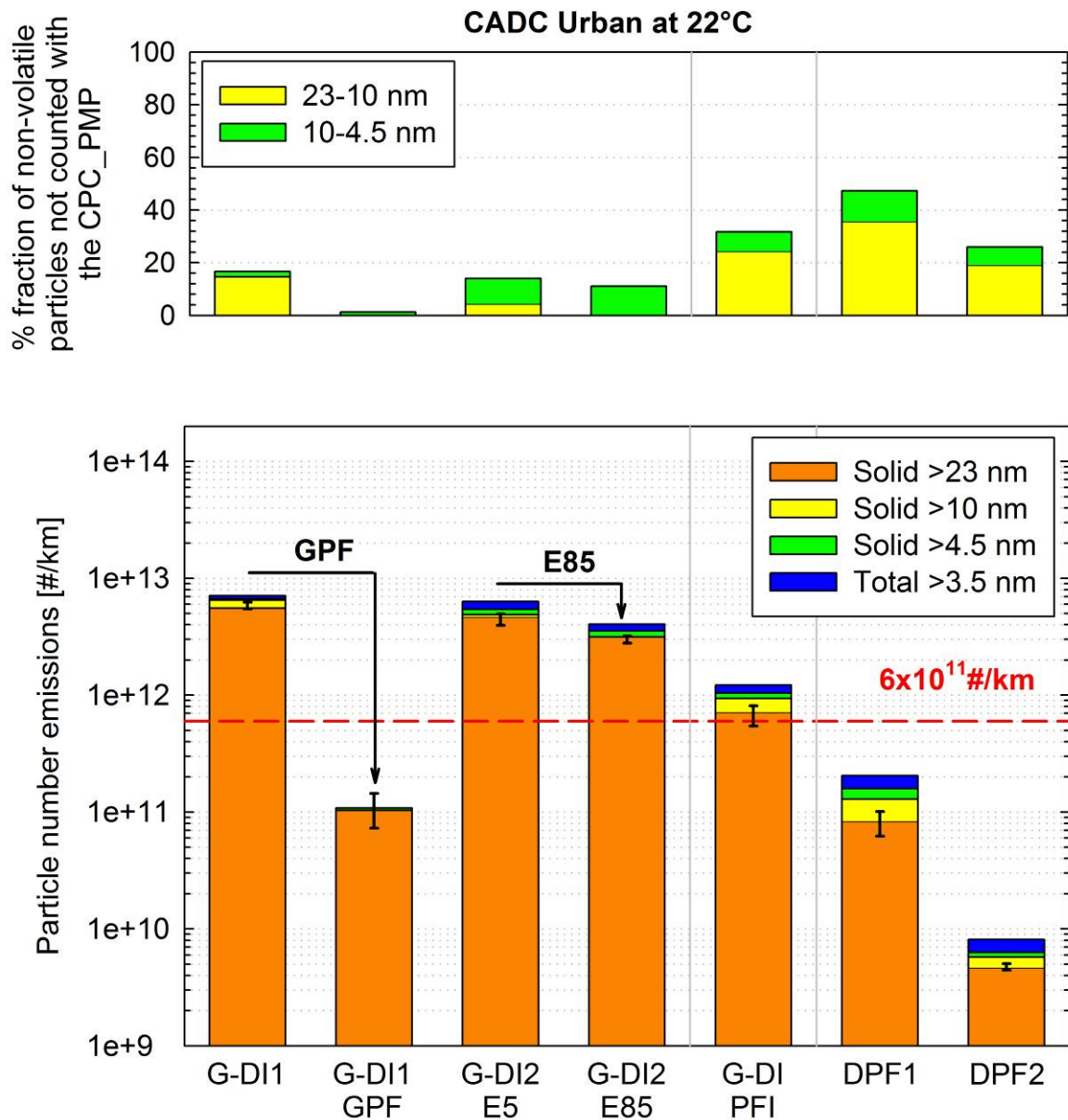


Figure 10: Particle number emission rates of the different vehicles tested over the urban phase of the CADC (bottom panel) and fraction of sub-23nm non-volatile particle counts not detected with the PMP CPC (top panel). Explanations as in Figure 6.

The GPF was more efficient in controlling the particle number emissions over the hot start CADC cycles. The filtration efficiency ranged from 96.6% over the motorway phase to 99.5% over the rural phase of the cycle, compared to 89% over the NEDC. This behaviour is very similar to that of wall flow filters in diesel applications, where it has been associated to either nucleation/condensation of previously stored semi-volatile material [31], or blowout of loose non-volatile particle deposits as the filter is exposed to highly transient operation with respect to the thermal and flow conditions [32], or even to small defects that close up as the DPF temperature rises [33].

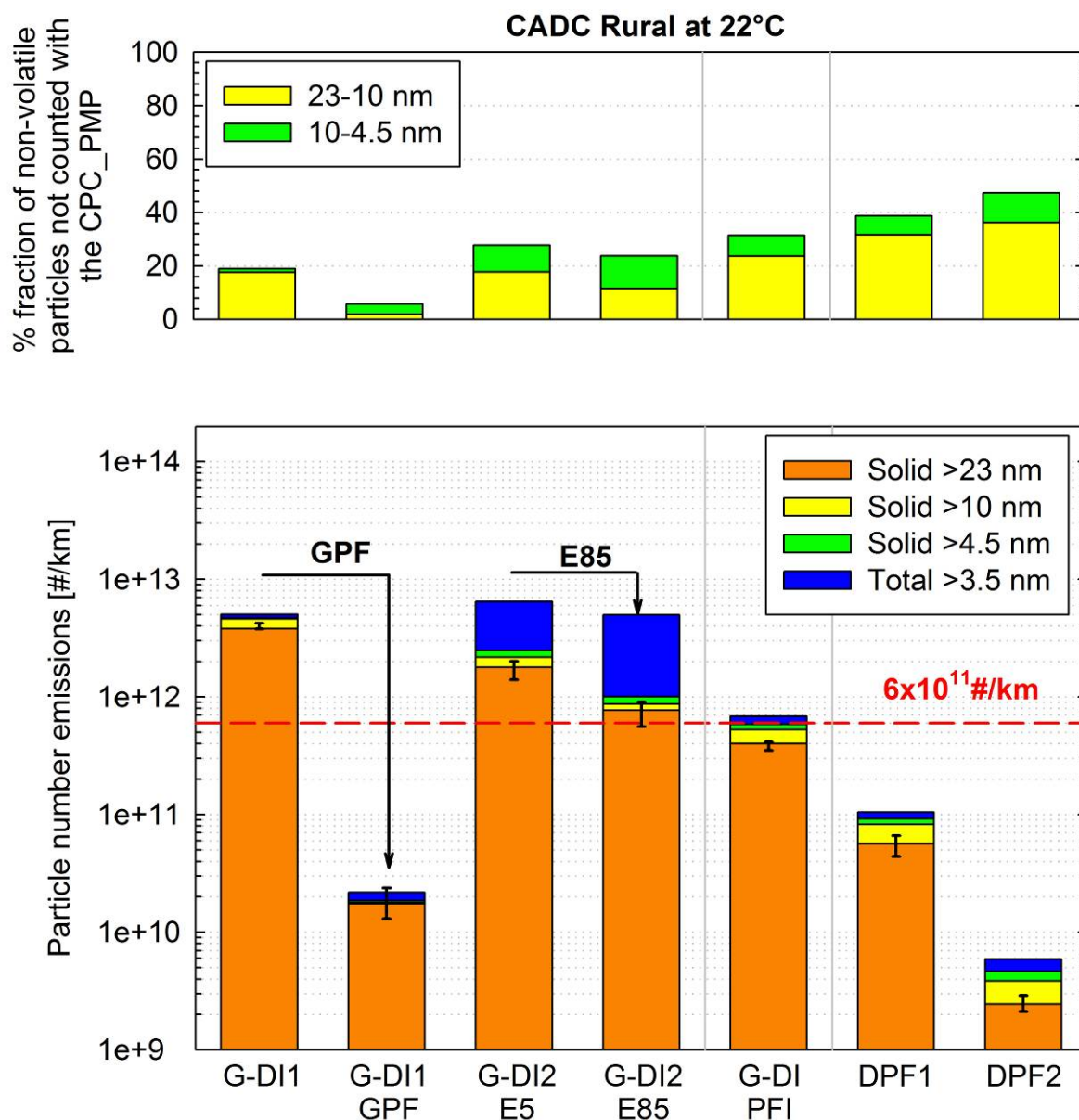


Figure 11: Particle number emission rates of the different vehicles tested over the rural phase of the CADC (bottom panel) and fraction of sub-23nm non-volatile particle counts not detected with the PMP CPC (top panel). Explanations as in Figure 6.

The beneficial effect of E85 on the particle number emissions of the FFV G-DI was also observed over the CADC test procedure. The emissions were reduced by 33% over the urban phase, 57% over the rural phase and 97% over the motorway part of the cycle. The reduction potential offered by ethanol is discussed in more details in section 4.4.2.

The G-DI/PFI hybrid exhibited a distinctly different behaviour from the conventional G-DI vehicles. Its particle number emissions were found to be at the diesel PN limit over all parts of the CADC cycle. On an average, it emitted  $7.1 \times 10^{11} \text{ #/km}$  ( $\pm 1.4 \times 10^{11} \text{ #/km}$ ) over the urban phase,  $4.0 \times 10^{11} \text{ #/km}$  ( $\pm 0.3 \times 10^{11} \text{ #/km}$ ) over the CADC rural and  $3.3 \times 10^{11} \text{ #/km}$  ( $\pm 0.6 \times 10^{11} \text{ #/km}$ ) over the motorway part. The particulate emissions of this vehicle will be discussed in more details in section 4.6.

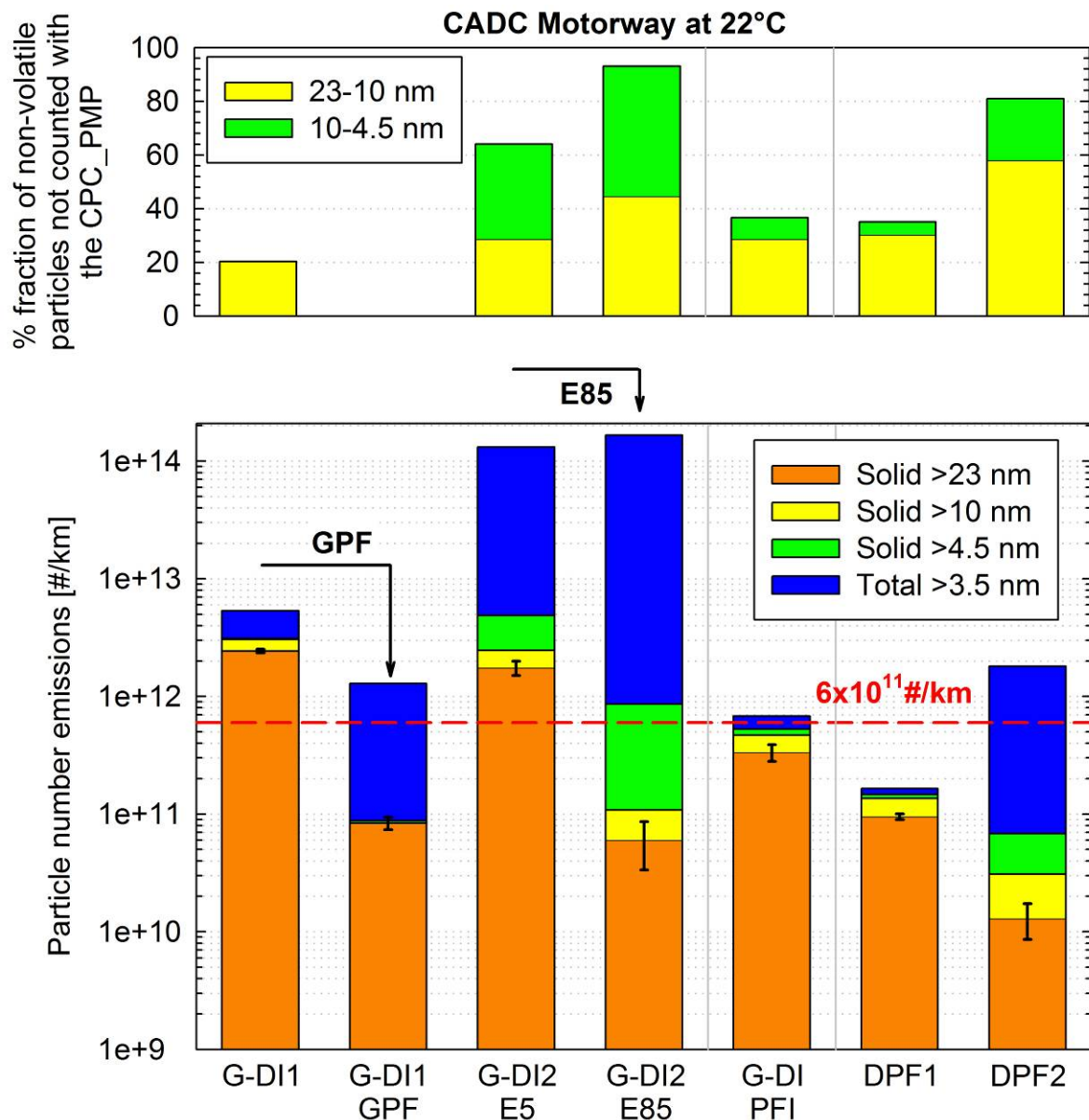


Figure 12: Particle number emission rates of the different vehicles tested over the motorway phase of the CADC (bottom panel) and fraction of sub-23nm non-volatile particle counts not detected with the PMP CPC (top panel). Explanations as in Figure 6.

The two DPF equipped diesels exhibited a distinctly different particle emission behaviour. The particle number emissions from DPF1 were relatively constant irrespective of the test cycle (from 0.6 to  $1 \times 10^{11}$  #/km). DPF2 on the other hand, emitted elevated particle concentrations over the cold start phase of the NEDC. Accordingly, the emissions over the different CADC phases were 72% (motorway) to 95% (rural) below those over NEDC. The different emission performance of the two DPF systems is evident in the real time traces shown in Figure 13 for two example NEDC tests with similar accumulated mileage on the DPF (~100 km after active regeneration). These results reflect differences in the DPF structure that are known to have a strong effect on the particulate emission performance [34].

With respect to the relative fraction of nano-sized particles not detected by the PMP CPC, the results over the urban and rural part of the CADC were quite similar to those over NEDC. A notable exception was the G-DI/PFI vehicle which appeared to have emitted a systematically higher fraction of nano-sized particles not counted by the CPC\_PMP. These results suggest that the lower emissions of this particulate vehicle over the CADC tests

compared to the regulated NEDC were associated with a shift towards smaller sizes (characteristic of lognormal distribution peaking at 38-40 nm).

The results over CADC motorway though showed a completely different picture. Under this driving condition, elevated levels of volatile particles were measured in the CVS tunnel. This was especially true for the G-DI2 and the DPF2 vehicles, where the total particle number emissions exceeded those determined in accordance to the regulated procedure by more than 3 (when using E85) and 2 orders of magnitude, respectively. During these particular tests, relatively higher particle counts were detected with the CPC@10 and (especially) the CPC@4.5.

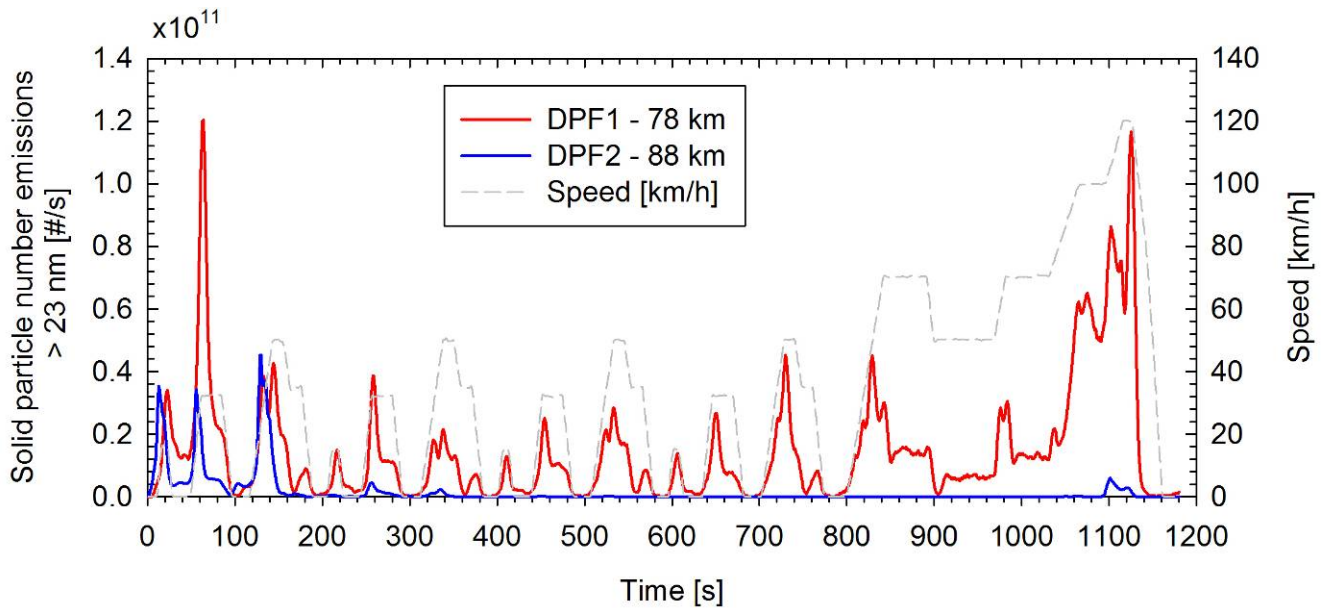


Figure 13: Comparison of particle number emission traces of the two DPF equipped diesels tested over the NEDC at 22°. The distances in the legend indicate the accumulated mileage since the last active regeneration of the DPF.

In order to get some more insight onto the nature of these nano-particles, tests were performed employing different dilution ratios. One particular concern was the possibility of re-nucleation of vapors downstream of the evaporating tube of the VPR system. Since the nucleation rates are a highly non-linear function of the vapour concentration it is anticipated that the use of elevated dilution ratios would suppress such volatile artifacts.

Figure 14 compares the real time traces of the different CPCs for two CADC motorway tests of the G-DI2 vehicle running on E5, where the primary dilution ratio was increased from 200 to 350. In both tests, very high emissions of volatile particles were recorded with the CPC@3.5, which actually got saturated over part of the cycle. The cycle-average CPC\_PMP results agreed within 20%, this difference lying within at the repeatability levels of the measurements conducted at the same PCRF value (~40%). The excess particles detected with the CPC@10 (57% vs 42%) and especially the CPC@4.5 (335% vs 115%), however, were higher when employing a lower dilution ratio. This is an indication that these particles are volatiles re-nucleating downstream of the VPR.

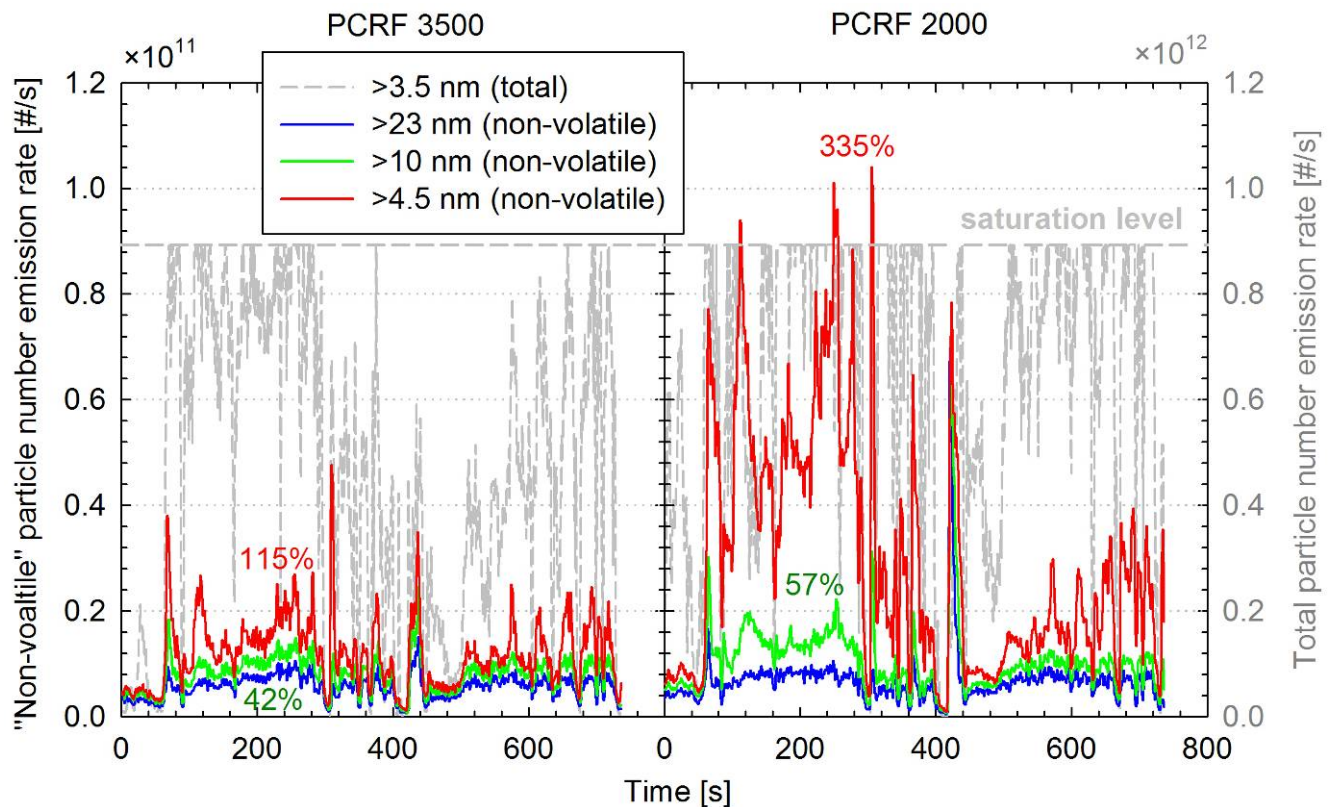


Figure 14: Real time emission rates recorded with the different CPCs in two tests of the G-DI2 vehicle running on E5, where different PCRF was employed in the VPR (3500 on the left hand panel and 2000 on the right-hand panel). The CPC\_PMP (blue lines), the CPC@10 (green lines) and the CPC@4.5 (red lines) were sampling downstream of the VPR while the CPC@3.5 (gray lines) was sampling thermally untreated aerosol directly from the CVS. Note that the total particle number emission rates (CPC@3.5) are scaled down by one order of magnitude (right-side axis). The percentage figures on the chart show the percentage difference of the cycle average (motorway) emissions determined with the CPC@10 (green font) and the CPC@4.5 (red font) relative to the CPC\_PMP results.

### 4.3 Effect of the test cell temperature

#### 4.3.1 PFI vehicles

The PFI1 and the PFI2 when running on gasoline were also measured over the NEDC at test cell temperatures of 15°C and 25°C. The results of these measurements are compared to those of the tests at 22°C in Figure 15 (PFI1) and Figure 16 (PFI2). The results suggested that there was a tendency towards elevated particle emissions over the ECE phase of the NEDC with decreasing test cell temperature. Yet due to the limited number of tests (two repetitions per test cell temperature) and the relatively large variability in the results at the same conditions, it is not possible to draw statistically significant conclusions.

One notable exception is that of the PFI2 vehicle when tested at 15°C which emitted twice as much particles over the ECE compared to the tests at 22°C. The elevated emissions were accompanied by a shift of the distribution towards larger particles, as evident from the fraction of nano-sized particles not detected with the CPC\_PMP which was almost half as much compared to that observed in the tests at 22 and 25°C.

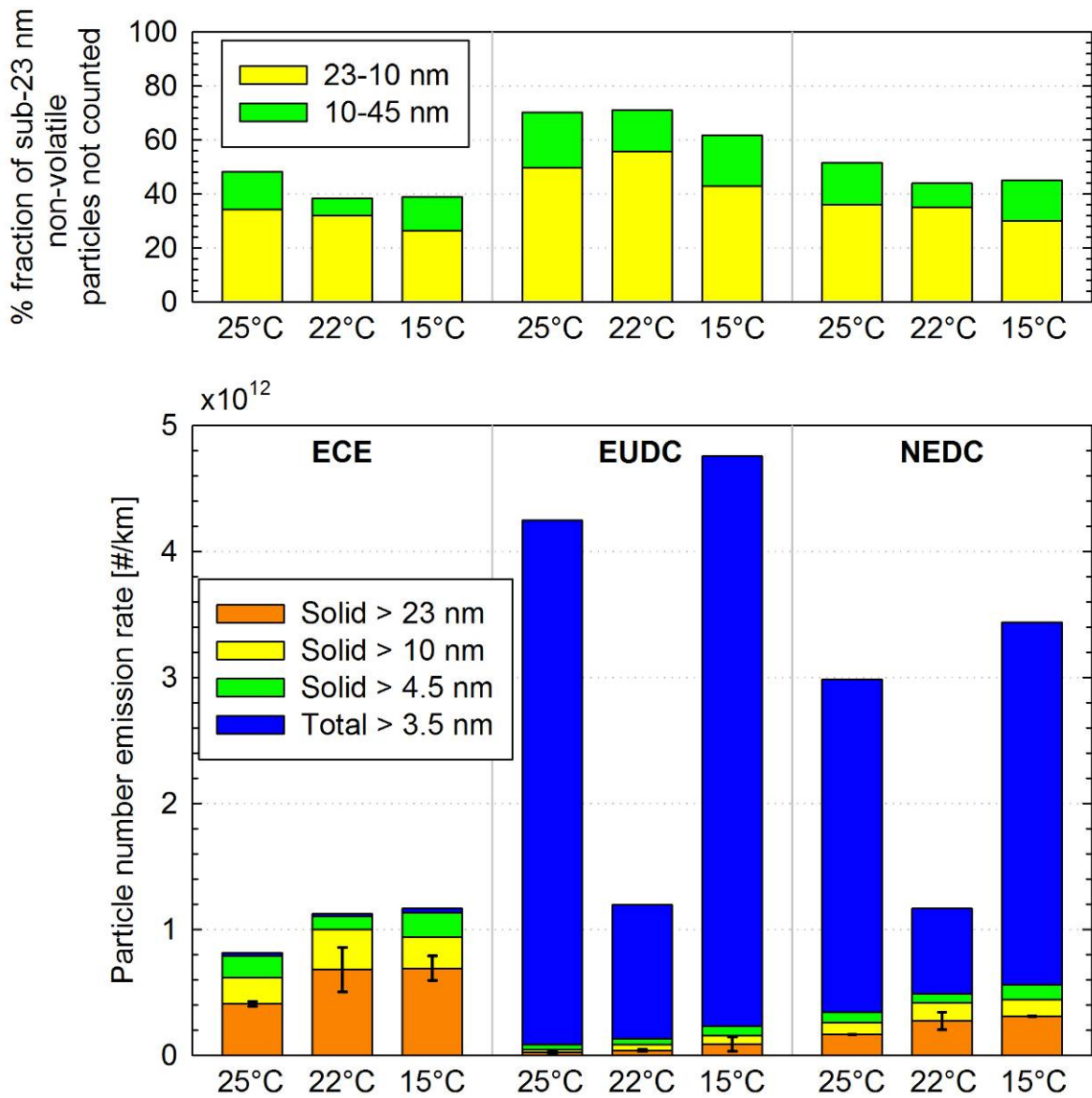


Figure 15: Particle number emissions of the PF11 vehicle (bottom panel) and fraction of sub-23nm non-volatile particle counts not detected with the PMP CPC (top panel) over the NEDC and its two phases (ECE and EUDC) at test cell temperatures of 25°C, 22°C and 15°C. Explanations as in Figure 6.

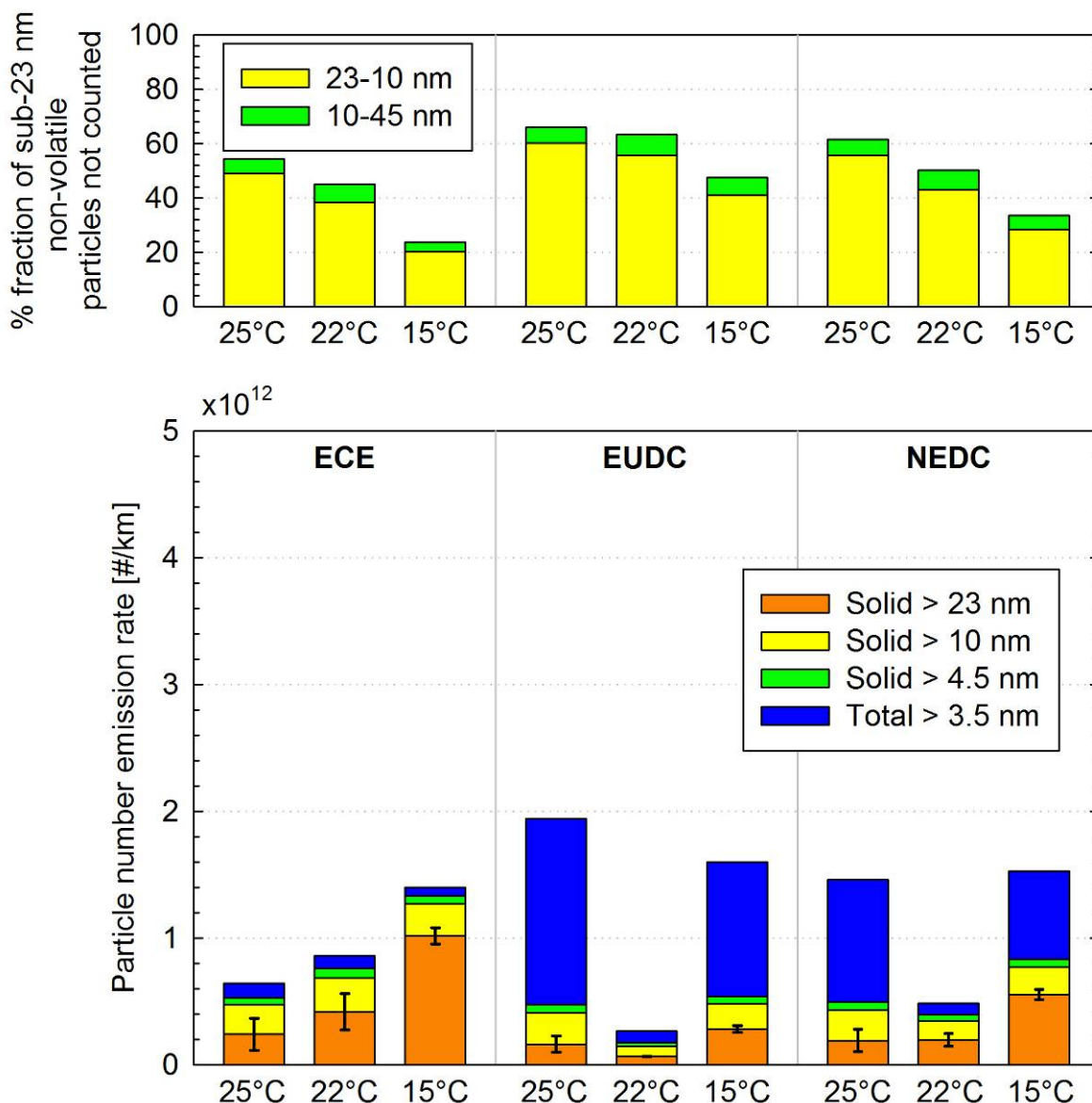


Figure 16: Particle number emissions of the PFI2 vehicle (bottom panel) and fraction of sub-23nm non-volatile particle counts not detected with the PMP CPC (top panel) over the NEDC and its two phases (ECE and EUDC) at test cell temperatures of 25°C, 22°C and 15°C. Explanations as in Figure 6.

## 4.3.2 G-DI vehicles

### 4.3.2.1 PM emissions

The G-DI vehicles were also measured at subzero (-7°C) test cell temperatures. Figure 17 compares the PM emissions at 22°C and -7°C over the NEDC. A five-fold increase was observed in the PM emissions of G-DI1 and the G-DI/PFI vehicle while an even higher increase (~570%) was observed for the G-DI2 running on E5, when tested at -7°C. All three vehicles exceeded the Euro 5 limit of 4.5 mg/km, with their emissions averaging at 6.8 mg/km ( $\pm 0.5$  mg/km – G-DI1), 4.6 mg/km ( $\pm 0.5$  mg/km – G-DI2 on E5) and 10.0 mg/km ( $\pm 0.3$  mg/km – G-DI/PFI). The GPF was 94% efficient at -7°C, and the emissions of the retrofitted G-DI1 vehicle were maintained at a 0.4 mg/km level. The use of E75 on the G-DI2 resulted also in a significant reduction of the PM emissions at -7°C, which averaged at 82%.

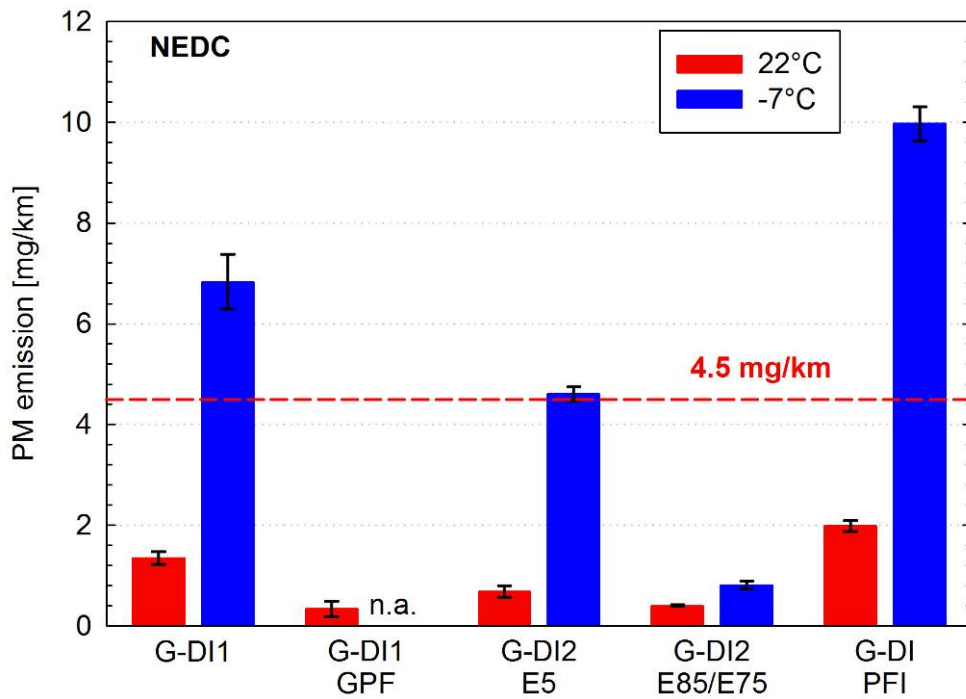


Figure 17: Average PM emissions of the different G-DI vehicles measured over the NEDC at 22°C (red bars) and -7°C (blue bars) test cell temperatures. Error-bars stand for  $\pm 1$  standard error.

The G-DI2 and the G-DI/PFI vehicles were tested at -7° also over the hot-start CADC procedure. Figure 18 compares the PM emissions over CADC at the two test cell temperatures examined. No emission deterioration could be identified for G-DI2 running on E5 and the G-DI/PFI vehicle, given the variability of the results. Interestingly, the use of E75 was even more beneficial at -7°C, effectively reducing the PM emissions of the G-DI2 to 0.64 mg/km ( $\pm 0.03$  mg/km). This corresponds to an 81% reduction over the CADC tests on E5 at -7°C, and a 63% reduction over the CADC tests on E85 at 22°C.

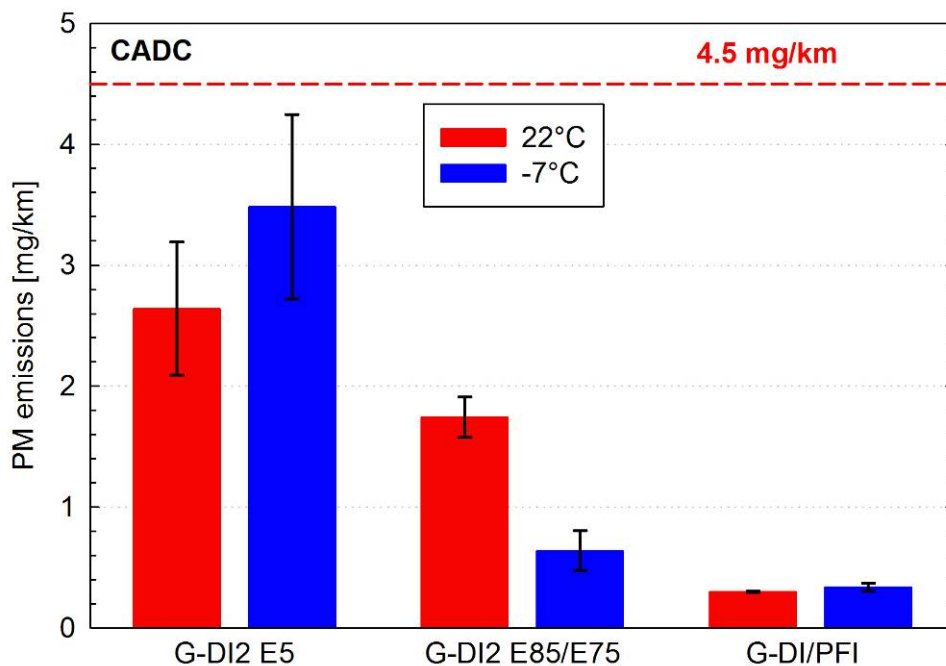


Figure 18: Average PM emissions of the different G-DI vehicles measured over the CADC at 22°C (red bars) and -7°C (blue bars) test cell temperatures. Error-bars stand for  $\pm 1$  standard error.

#### 4.3.2.2 Particle number results

Figure 19 compares the particle number emissions of the G-DI1 vehicle over NEDC tests at 22°C and -7°C. Operation of the vehicle at sub-zero temperatures increased the particle number emissions over the ECE part of the cycle by 220% but had no effect on the emissions over the EUDC phase. This behaviour is indicative of excess emissions during cold start, as evident in Figure 20 plotting the real time traces of particle number emissions together with the calculated lambda from the gaseous emissions. The fuel over-enrichment was extended from 30 s to almost 220 s when the test cell temperature dropped from 22°C to -7°C. This had a profound effect on the particle number emissions which were 3.5 times higher over the first ECE15 elementary cycle in the sub-zero tests. Yet increased emissions were observed over the following two ECE15 phases (2<sup>nd</sup> and 3<sup>rd</sup>), being 2.75 and 1.95 times higher, respectively, in the sub-zero temperature tests.

The elevated emissions were accompanied by an increase of the particle sizes as suggested by the nearly identical indications of the three CPCs sampling downstream of the VPR over the entire ECE part of the cycle.

Similar behaviour was observed in all G-DI vehicles tested. For example, Figure 21 compares the particle emissions of the G-DI2 vehicle running on E5 over NEDC and CADC tests at 22°C and -7°C. The NEDC results at 15°C are also included in the figure. Again the operation at sub-zero temperatures resulted in an increase of particle numbers over the ECE part of the NEDC (166% increase) but had no effect on the emissions over EUDC and the hot-start CADC cycles. A similar but less pronounced effect was observed in the tests at 15°C, with the NEDC emissions averaging at  $3.1 \times 10^{12}$  #/km ( $\pm 1.1 \times 10^{11}$  #/km) compared to  $2.2 \times 10^{12}$  #/km ( $\pm 2.7 \times 10^{11}$  #/km) at 22°C.

Again the increase of the particle number emissions over the ECE part at the -7°C tests was accompanied by an increase of the particle size. The CPC\_PMP was measuring the same concentrations with the CPC@10 and missed only 4% of the particle counts detected with the CPC@4.5, over the particular test cycle.

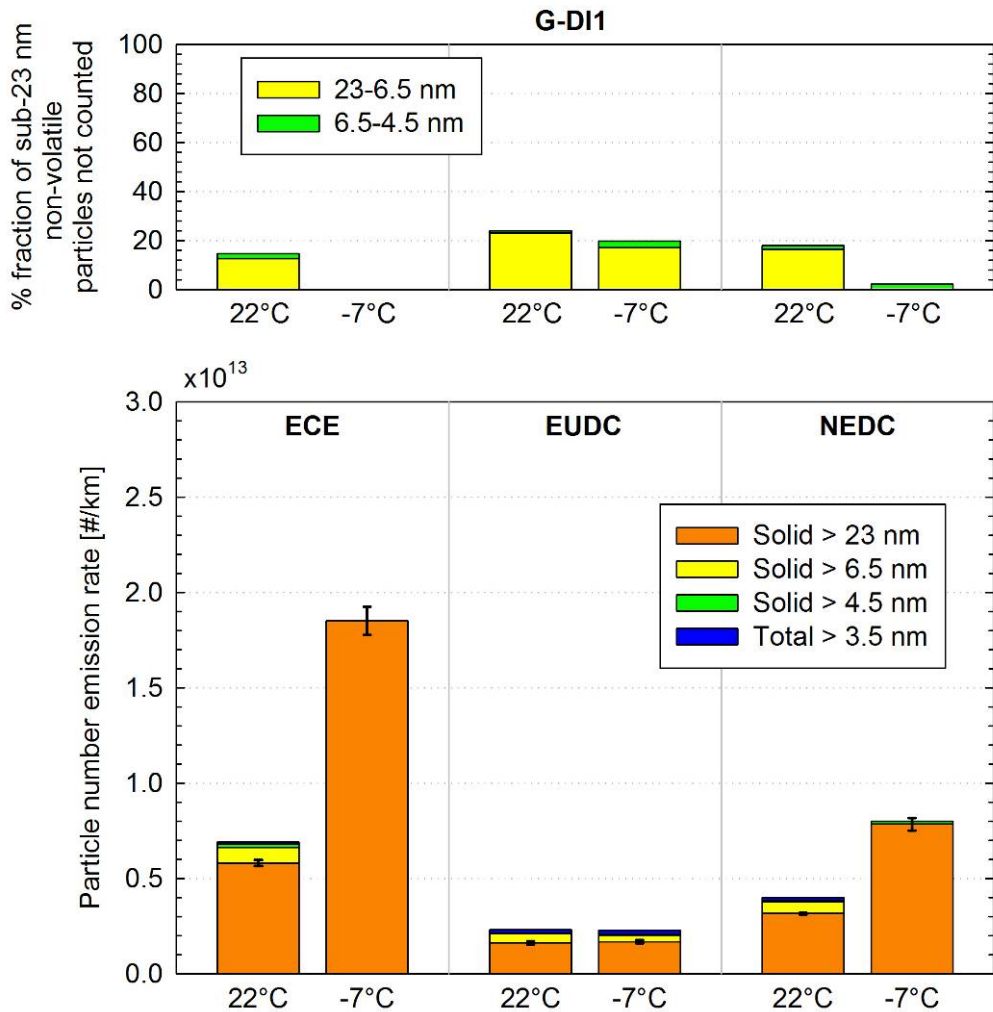


Figure 19: Average particle number emissions of the G-DI1 vehicle (bottom panel) and fraction of sub-23nm non-volatile particle counts not detected with the PMP CPC (top panel) over the NEDC and the two phases of the cycle, at 22 and -7°C test cell temperature. Explanations as in Figure 6.

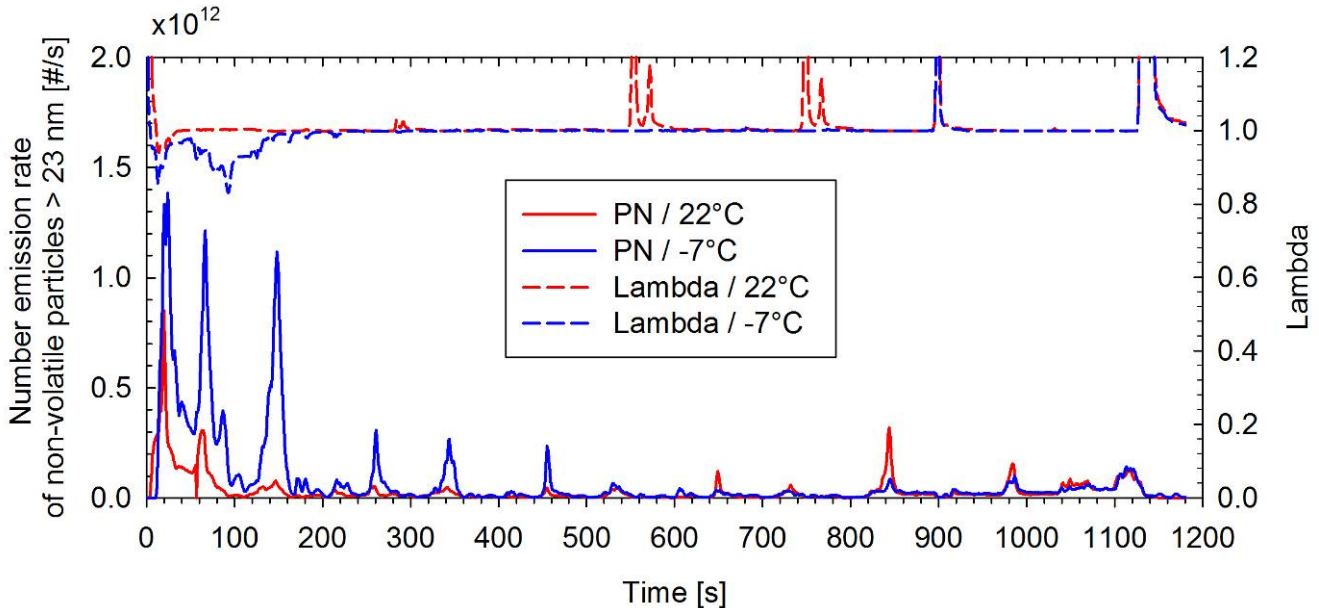


Figure 20: Real time emission rates of “non-volatile” particles (solid lines) measured in accordance to the European regulation and calculated lambda (dotted lines) for two NEDC tests of the G-DI1 vehicle at 22°C (red lines) and -7°C (blue lines).

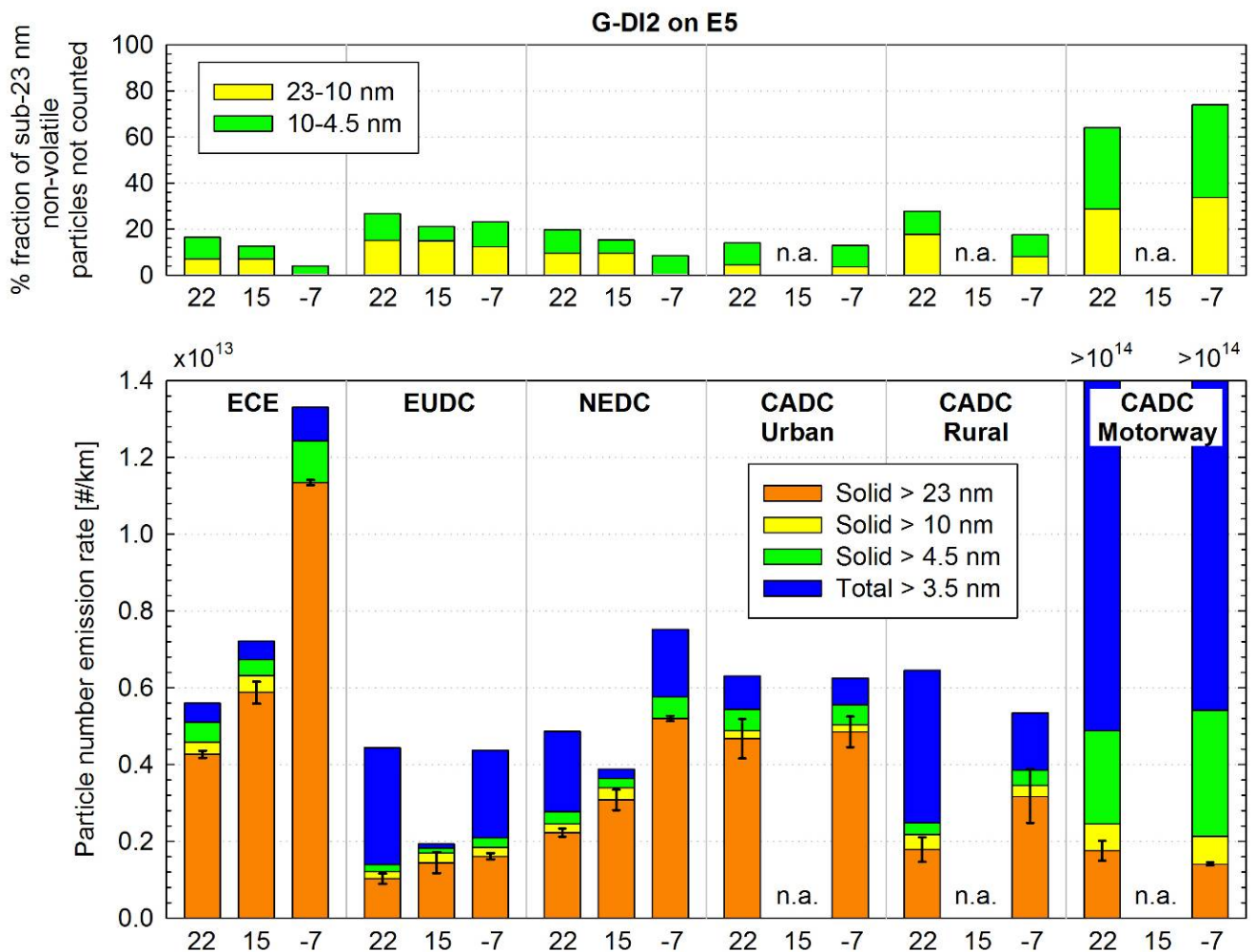


Figure 21: Average particle number emissions of the G-DI2 vehicle (bottom panel) and fraction of sub-23 nm non-volatile particle counts not detected with the PMP CPC (top panel) over the NEDC and the CADC, at 22°C, 15°C and -7°C test cell temperature. Explanations as in Figure 6.

## 4.4 Effect of fuel

### 4.4.1 Use of CNG on PFI2

No clear effect of the CNG/H<sub>2</sub> formulation on the solid particle number emissions could be observed (Figure 22), with the results showing a rather large variability. Interestingly, elevated emissions of volatile particles were measured when using CNG of G25 quality. The majority of these particles were formed over the last part of the EUDC phase, where the CPCs sampling downstream of the VPR remained at background levels. The use of G25 CNG fuel resulted also in systematically higher Total HydroCarbon (THC) emissions over the EUDC, which as in the case of the volatile particle number, occurred mainly over the last part of the cycle even if the three way catalyst was warm (onset of Figure 23). Yet no clear correlation between THC and total particle number could be established.

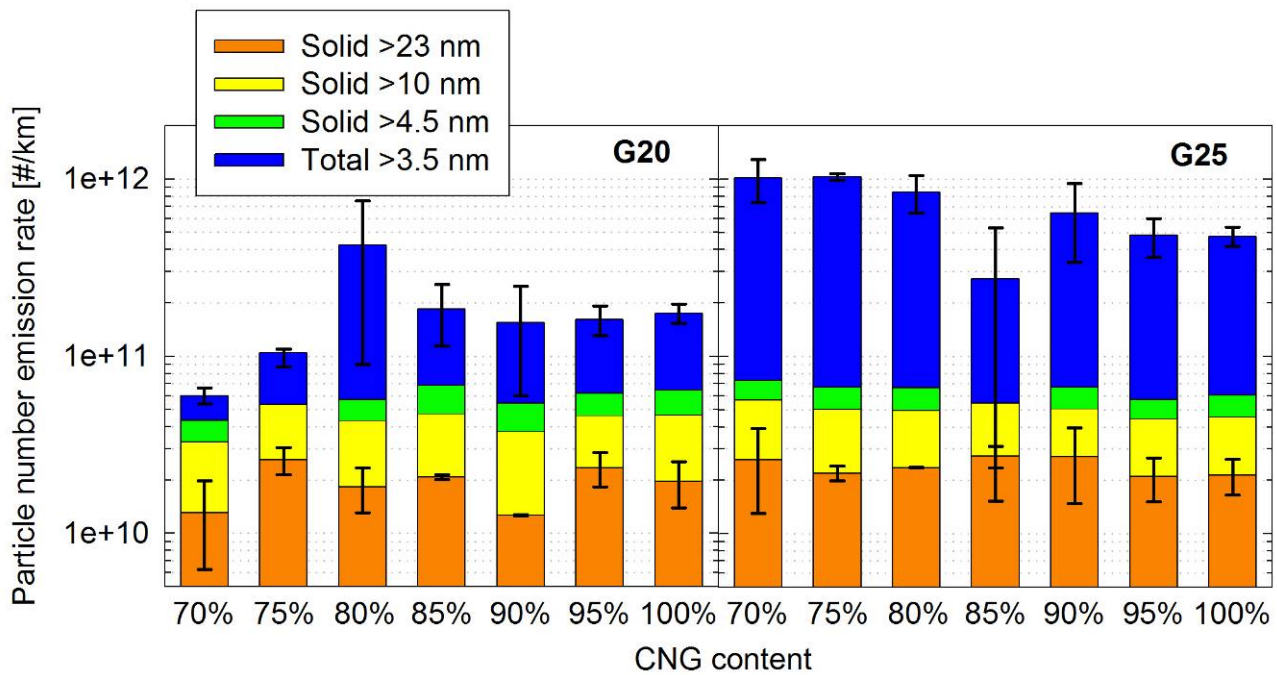


Figure 22: Particle number emission rates of the PF12 vehicle over the NEDC when running on CNG/H<sub>2</sub> mixtures as a function of the CNG content. Results are shown separately for tests with CNG of G20 (left-hand panel) and G25 (right-hand panel) quality. Explanations as in Figure 6.

Sulphates have been identified to promote nucleation mode formation in both theoretical [35] and experimental [36, 37] studies, owing to the very low vapour pressures. Release of sulphates stored in the TWC requires elevated exhaust temperatures that may have occurred over the EUDC part of the cycle, and may even be enhanced in the presence of hydrogen [38]. Hydrocarbons can then condense on the nucleated sulphate particles thus growing into large enough sizes to be detected by CPCs. Nucleation is also enhanced in the absence of a solid particle core onto which the precursors may condense. In that respect, the higher nucleation rates observed when using G25 CNG might indicate a higher sulphur content on the G25 CNG. However, this information is not available.

The solid particle number emissions of this Bi-Fuel vehicle, when running on CNG/H<sub>2</sub> mixtures, were generally found to be at the background levels with the exception of a spike occurring at the first 40 s of the cycle (e.g. Figure 24 but also evident in the total particle emissions shown in the onset of Figure 23). This burst of particle emissions is most probably associated with the operation of the vehicle on gasoline during start up, an approach commonly employed to avoid ice forming on the pressure regulator.

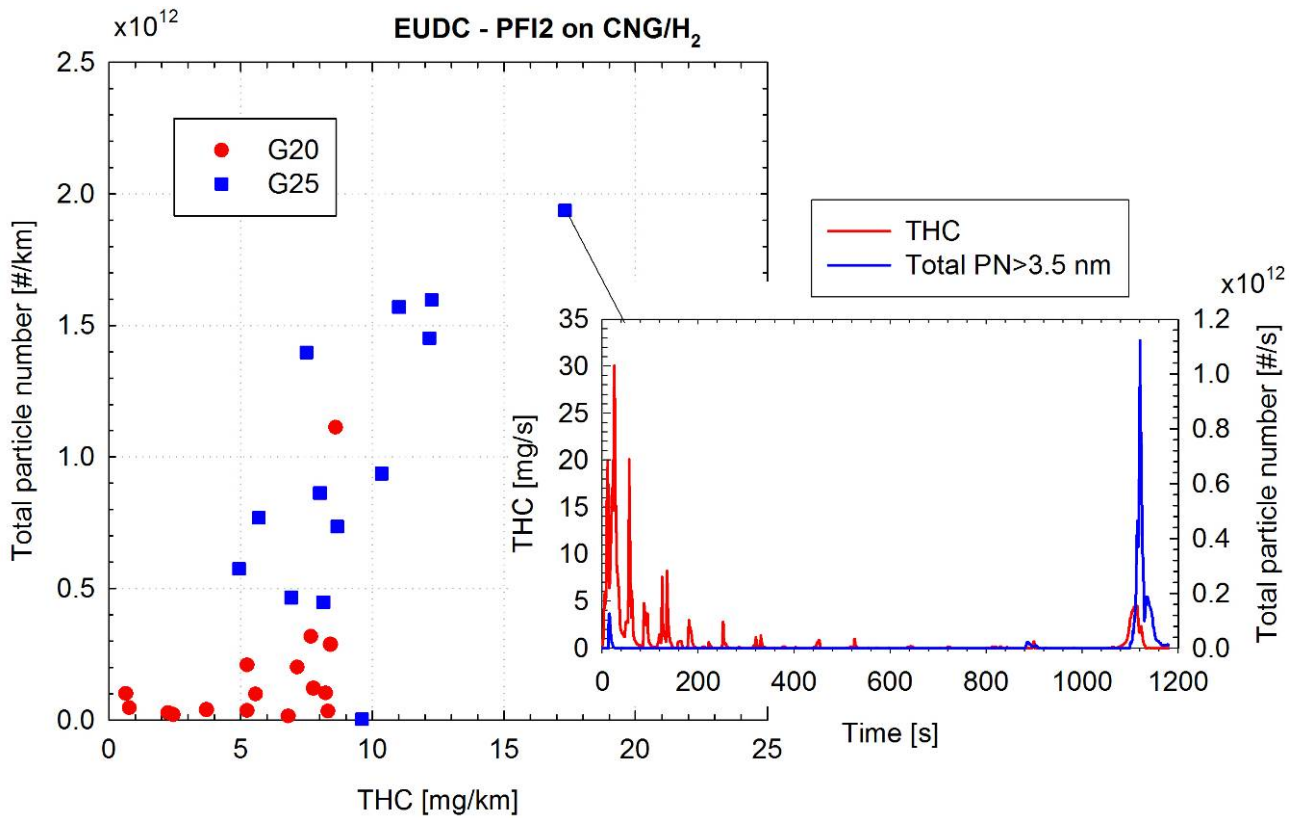


Figure 23: Comparison of the total particle number and Total HydroCarbon (THC) emissions of the PFI2 vehicle over the EUDC when tested on CNG/H<sub>2</sub> mixtures with G20 (red symbols) and G25 (blue symbols) CNG. The onset shows the real time traces of THC and total particle number for the test where the vehicle exhibited the highest emissions.

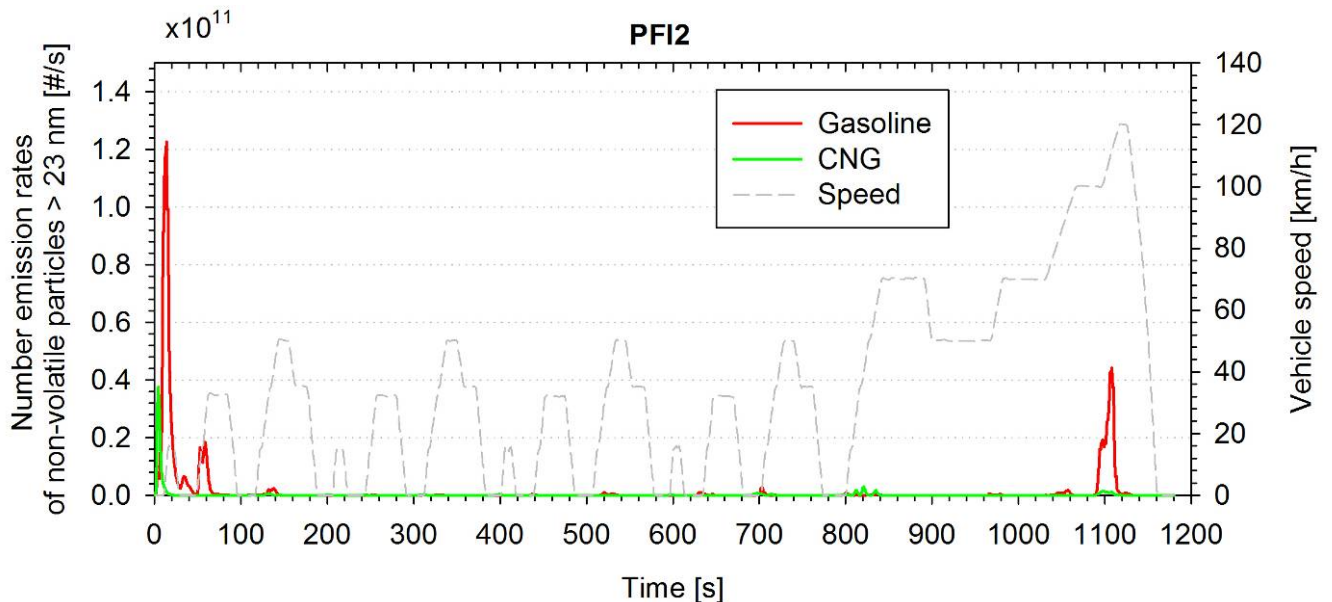


Figure 24: Comparison of the nonvolatile particle number emission rates > 23 nm of the PFI2 when tested over NEDC with gasoline (red line) and G20 CNG (green line).

#### 4.4.2 Use of E75/E85 on G-DI2

The use of E85 (22°C) and E75 (-7°C) fuel on G-DI2 resulted in a systematic reduction of the non-volatile particle number emissions under all driving conditions. The actual reduction depended on the operating conditions (Figure 25). Under hot-start, real-world driving the reduction was highest under motorway driving (>95%) and lowest under urban driving conditions (33% for E85 and 19% for E75). The effect of high ethanol blends was broadly similar over the CADC Rural and the EUDC part of the NEDC (approximately 60% for E85 and 80% for E75). A large reduction (47% for E75 and 67% for E85) was also observed over the cold start ECE. No consistent effect of the test cell temperature could be identified, with the reductions being higher at 22°C under urban driving but lower under rural driving (CADC rural and EUDC).

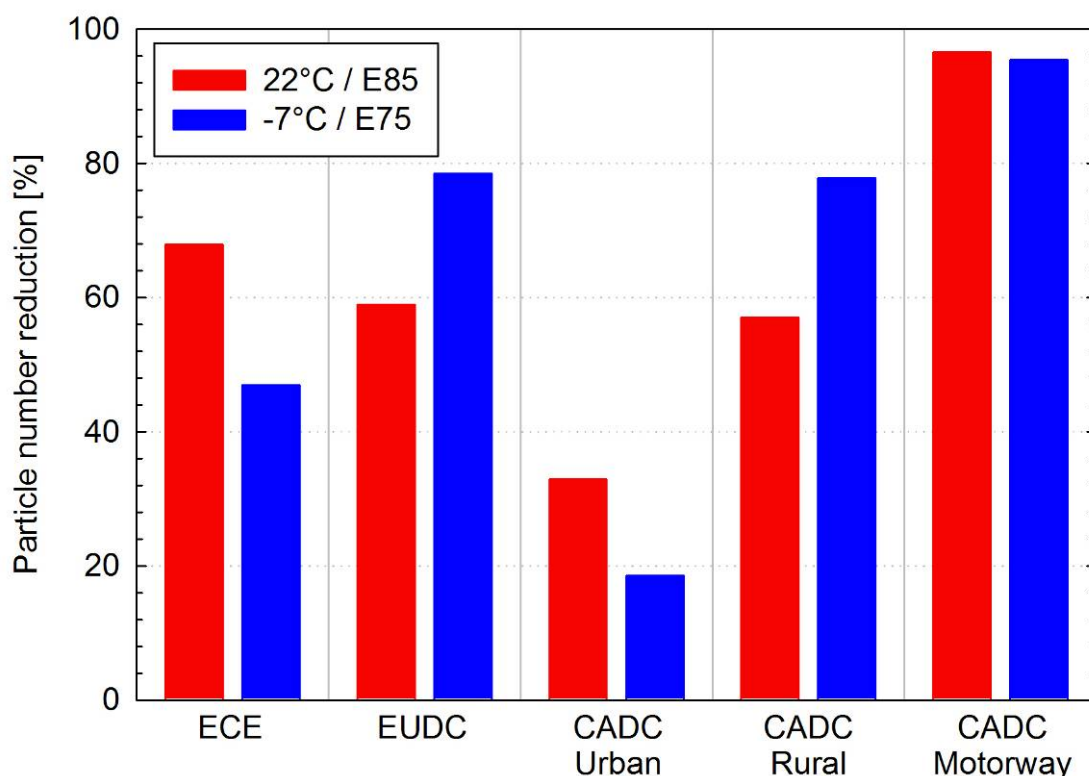


Figure 25: Percentage reduction in the particle number emissions measured in accordance to the PMP methodology by the use of E85 (red bars) and E75 (blue bars) over the main phases of the NEDC and CADC.

The real time traces of the particle number emissions provide some additional insight onto the emission reduction potential offered by the use of fuels with high ethanol content. Figure 26 and Figure 28 compare the particle number emission rates at both 22°C and -7°C over the NEDC and the CADC, respectively. The real time data indicate that the emission reduction is higher over cold start operation and high speed driving (especially above ~100 km/h).

The high emission reduction potential of E85 has been reported in several recent publications. Szybist et al. [20] also observed a 1 to 2 orders of magnitude reduction in the particle number emissions in a 2 l G-DI engine tested at high load (8 bar imep) when running on E85 compared to gasoline or 20% ethanol/gasoline blends. Large reductions, but smaller in magnitude (in the order of 70%), were reported by Lee et al. [22] in tests at lower loads (4 and 6.3 bar imep) for a late technology single cylinder spray-guided direct injection engine when running on E85.

The particle emission reduction resulting from the use of high ethanol fuels was attributed to the lower sooting tendency of ethanol, originating from a) the presence of ~30% oxygen bound in the ethanol molecules helping particle oxidation, b) the lack of isomers, alkenes and aromatics (present in gasoline) which are known to produce more soot particles but also c) the lower content in less volatile gasoline fractions [21]. Yet, the lower heating value and the higher latent heat of vaporization of ethanol necessitates the injection of higher quantities of fuel when using E85 that can result in more frequent piston wetting and longer vaporization times [20], that are known to promote soot formation. The relative merits of ethanol are therefore expected to depend on the fuel-injection strategy and effectively on the engine operating conditions.

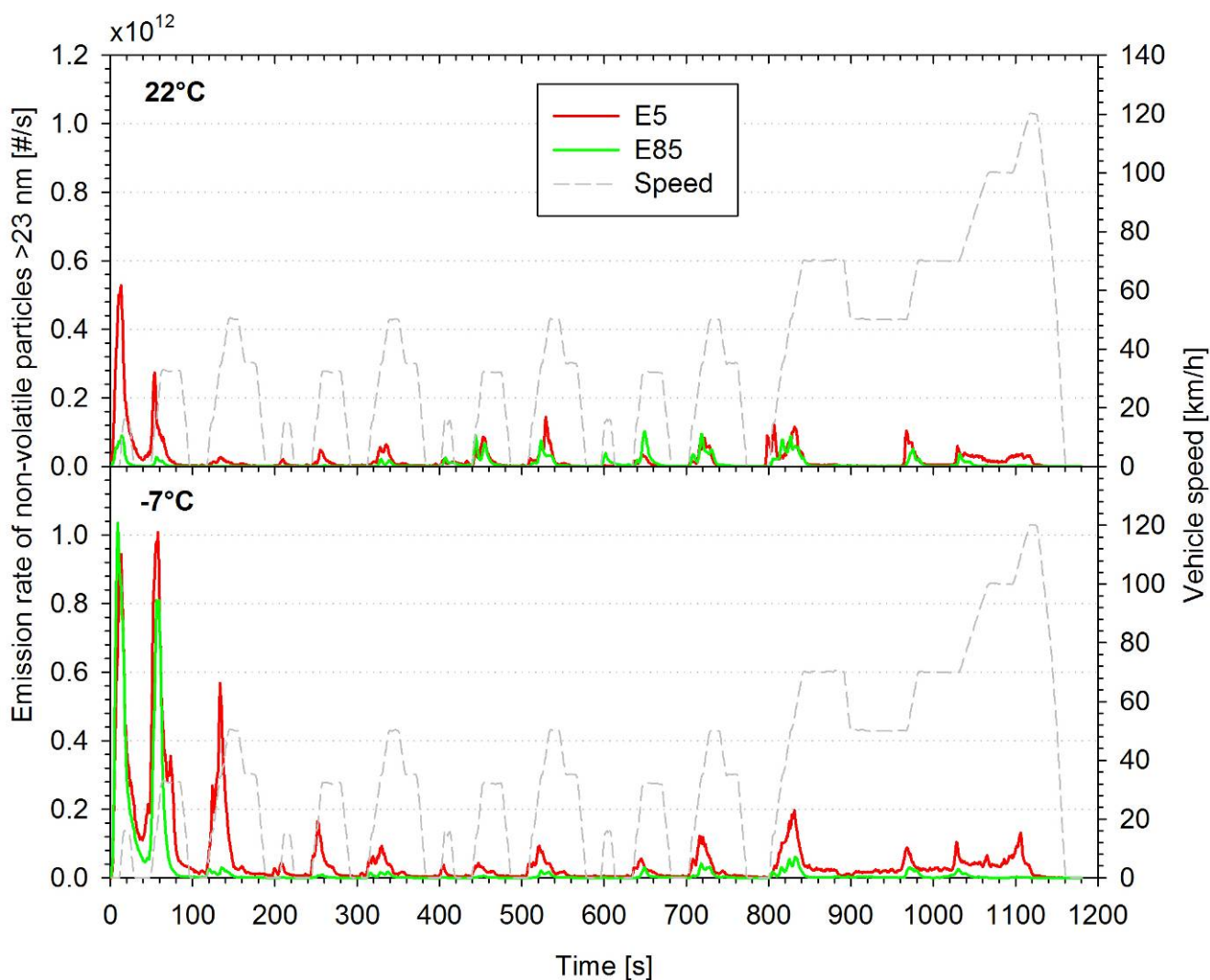


Figure 26: Real time traces of non-volatile particles >23 nm emitted by G-DI2 over the NEDC when running on E5 (red line) and E85 (green line) at test cell temperatures of 22°C (top panel) and -7°C (bottom panel).

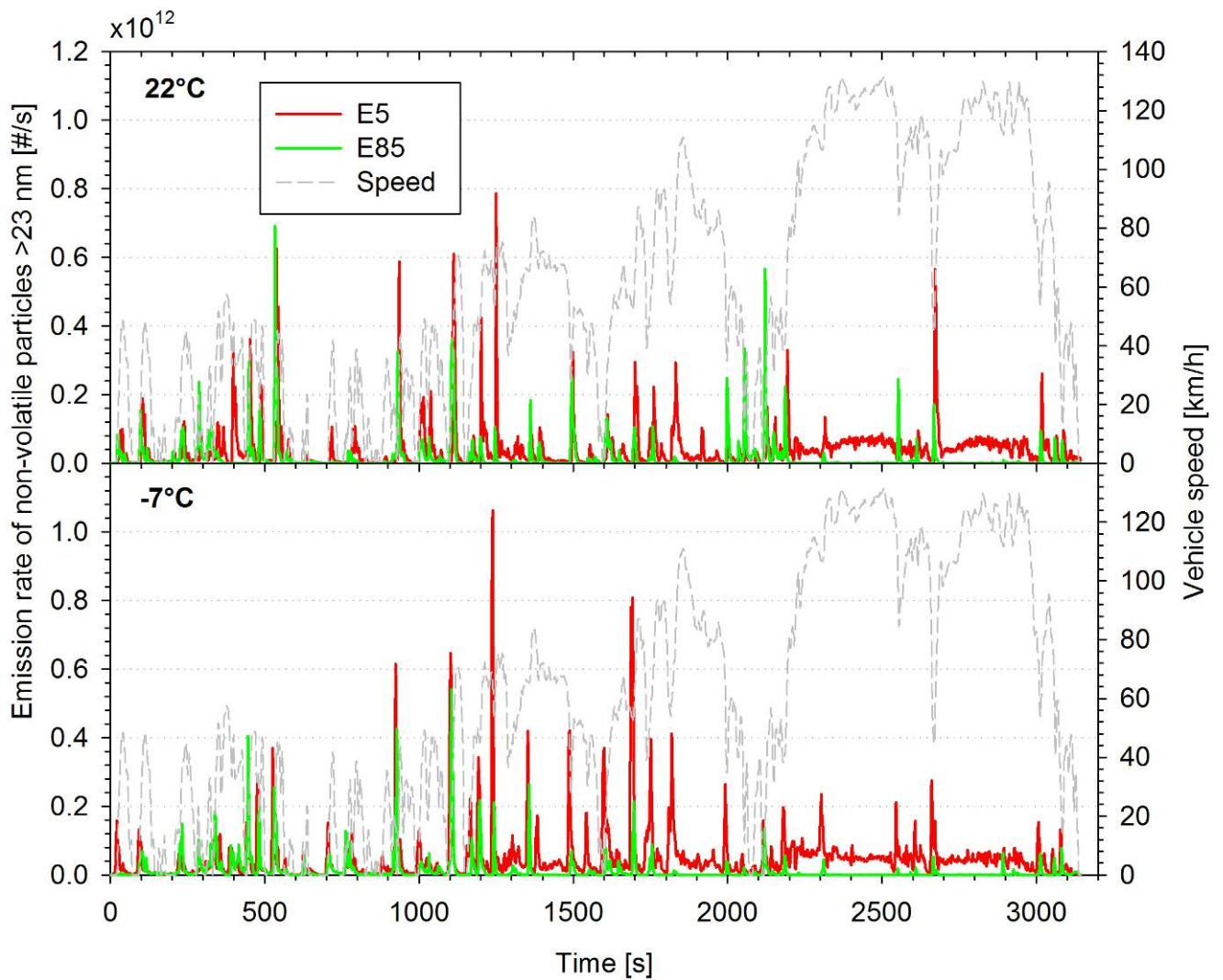


Figure 27: Real time traces of non-volatile particles >23 nm emitted by G-DI2 over the CADC when running on E5 (red line) and E85 (green line) at test cell temperatures of 22°C (top panel) and -7°C (bottom panel).

The measured size distributions in the studies of Szybist et al. [20] and Lee et al. [21] also suggest that the use of E85 results in a shift of the size distribution towards smaller particle sizes. Such a shift was not evident in the G-DI2 results. For example Figure 28 compares the fraction of particles measured downstream of the VPR with the CPCs having a lower  $d_{50}$  that were not detected by the PMP CPC. No clear effect could be identified by the use of high ethanol fuel in either the 22°C or the -7°C tests.

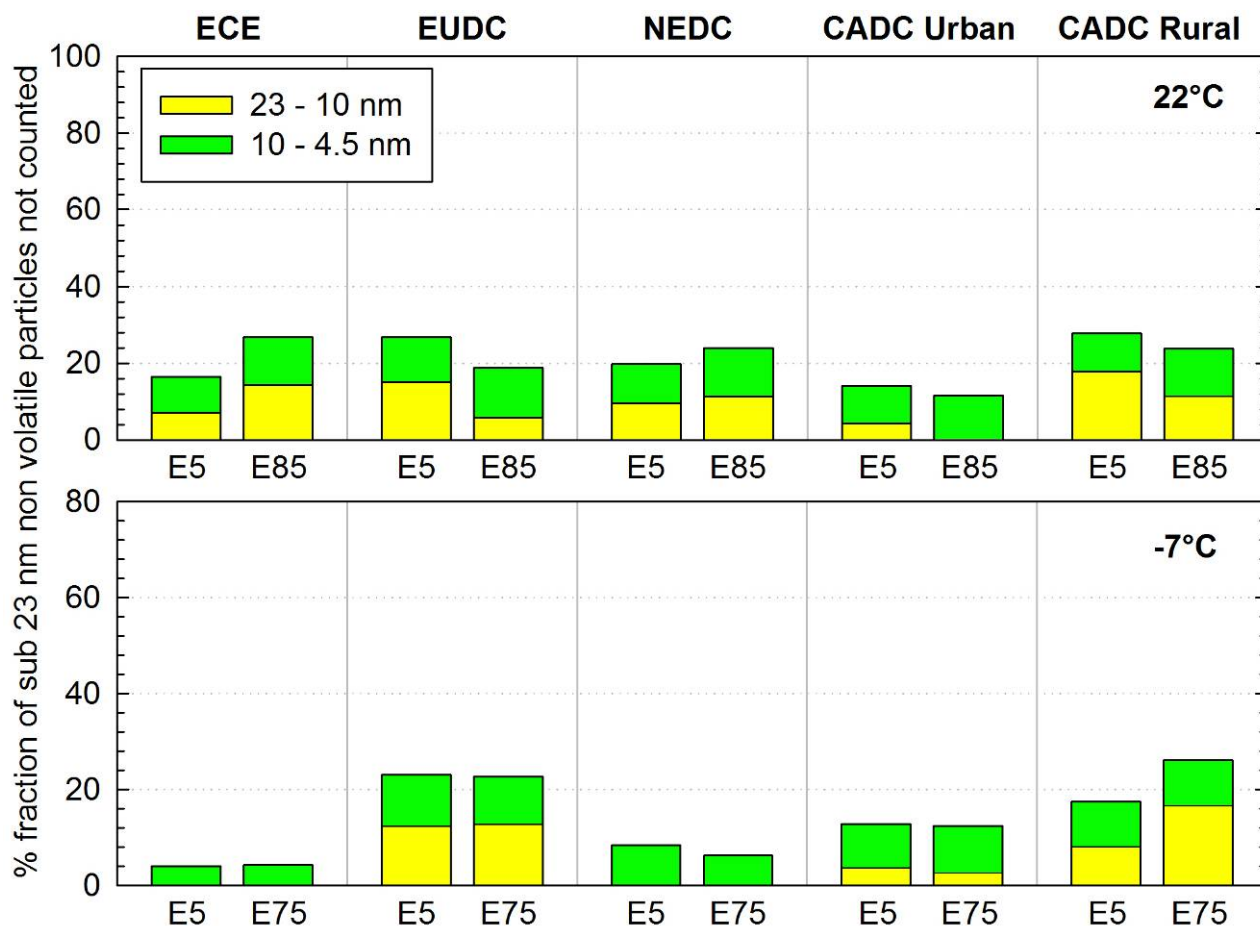


Figure 28: Average fraction of sub-23 nm non-volatile particle counts not detected with the PMP CPC over the NEDC and the CADC tests of the G-DI2 running on E5 and E75/E85, at 22°C (top panel) and -7°C (bottom panel) test cell temperature. No results are shown for the motorway part of the CADC, due to the observed volatile artifact (e.g. Figure 14).

#### 4.5 GPF performance

The installation of the GPF on G-DI1 was found to be very efficient in controlling the emitted number of non-volatile particles. Figure 29 summarizes the average filtration efficiencies over the different cycles tested at 22°C with the three CPCs sampling downstream of the VPR. Over the EUDC phase of the NEDC cycle and all phases of the CADC, the filtration efficiency was found to be systematically above 95% with all CPCs employed. A somehow lower filtration efficiency was observed over the ECE averaging at 86%, based on the indications of the PMP compliant CPC. This deterioration of the filtration efficiency over the cold start phase of the NEDC is shown more clearly in Figure 30 which compares the real time particle emission rates with and without GPF. Similar behaviour is commonly observed in wall-flow filters for diesel applications and has been associated to either nucleation/condensation of previously stored semi-volatile material [31], or blowout of loose non-volatile particle deposits as the filter is exposed to highly transient operation with respect to the thermal and flow conditions [32], or even to small defects that close up as the DPF temperature rises [33].

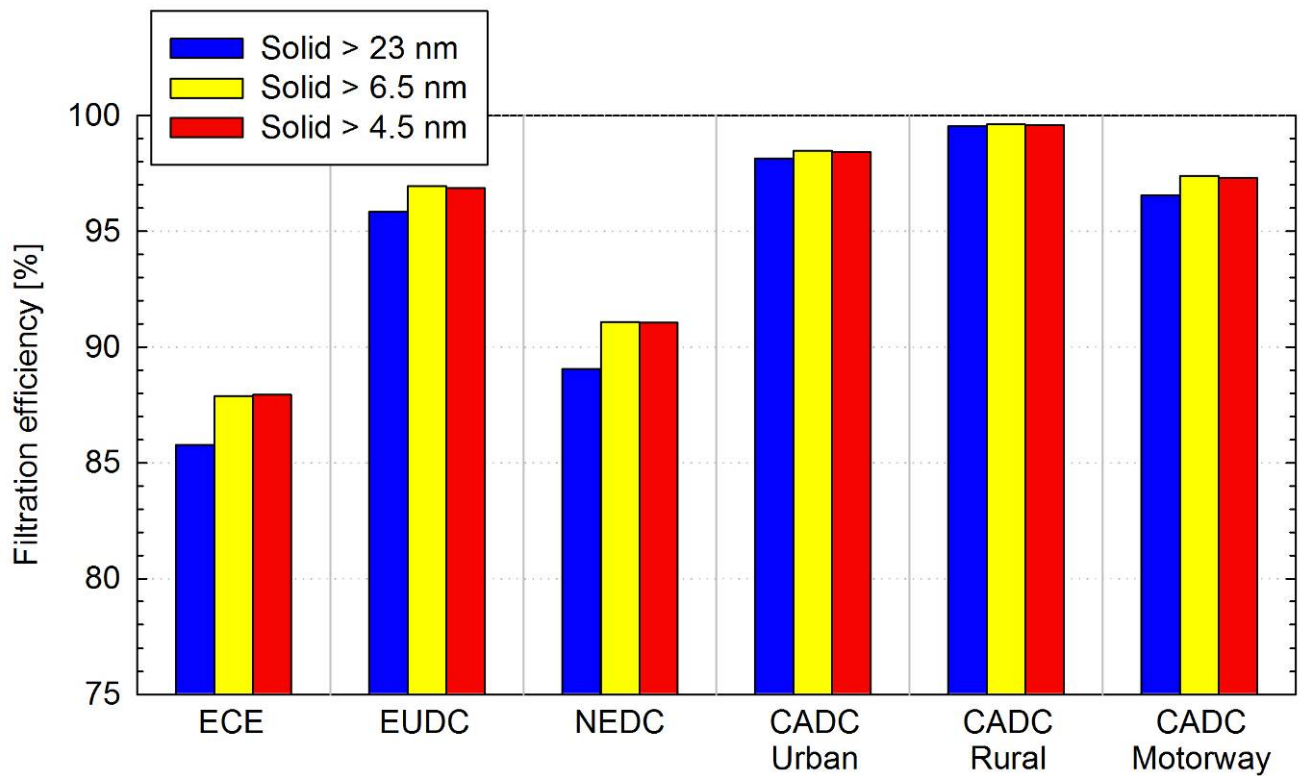


Figure 29: Average filtration efficiency of the GPF over the NEDC and CADC as determined with the different CPCs sampling downstream of the VPR.

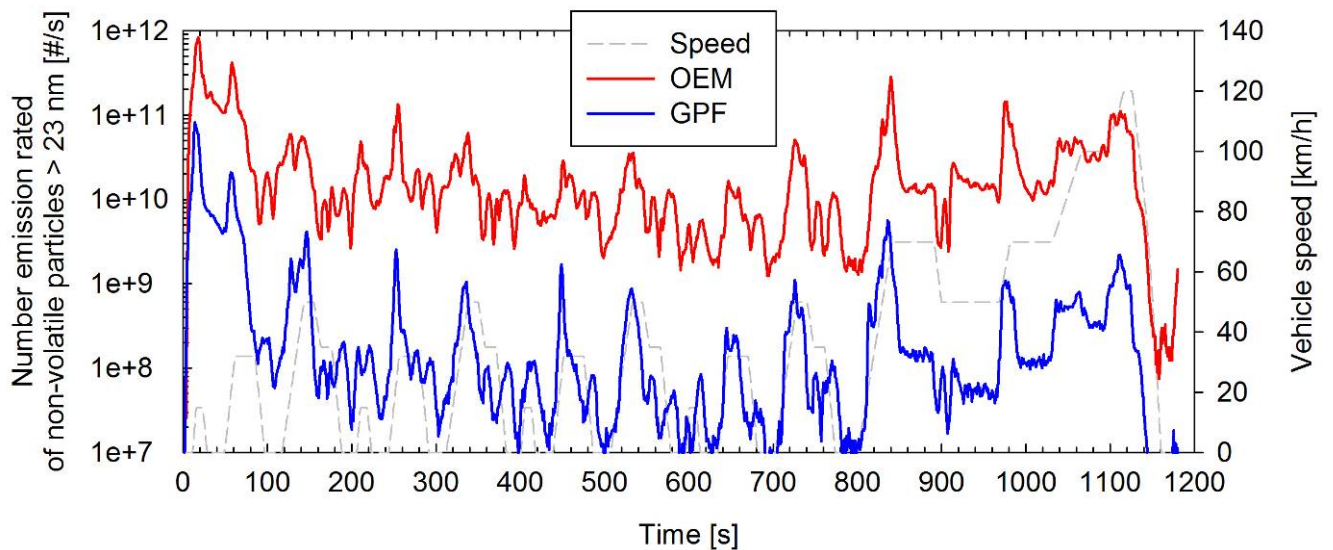


Figure 30: Real time number emission rates of non-volatile particles > 23 nm from G-DI1 tested with (blue line) and without (red line) GPF over the NEDC at 22°C.

The GPF was also found to be more efficient in controlling smaller particles. This is reflected in the systematically higher filtration efficiencies determined with the CPCs having a lower cut-off size (Figure 29). This is also evident in the number weighted mobility size distributions over the steady state tests, plotted in Figure 31. The measured distributions in the tests without a GPF were rather broad, being skewed towards small sizes. Even if the

samples were drawn from the CVS tunnel, the total number concentrations derived from the SMPS distributions agreed within 10% with the non-volatile number concentrations measured with the CPC@4.5. These differences are within the expected accuracy of the SMPS number concentrations [39], and therefore suggest that there was no distinct volatile mode present. Any adsorbed or condensed volatile material onto the solid particles would only result in an overestimation of the non-volatile particle sizes. The size distributions measured when the vehicle was retrofitted with the GPF were much narrower and peaked to a larger size, although to a certain extent this might just reflect the lower sensitivity of the SMPS to smaller sizes at such low concentration levels.

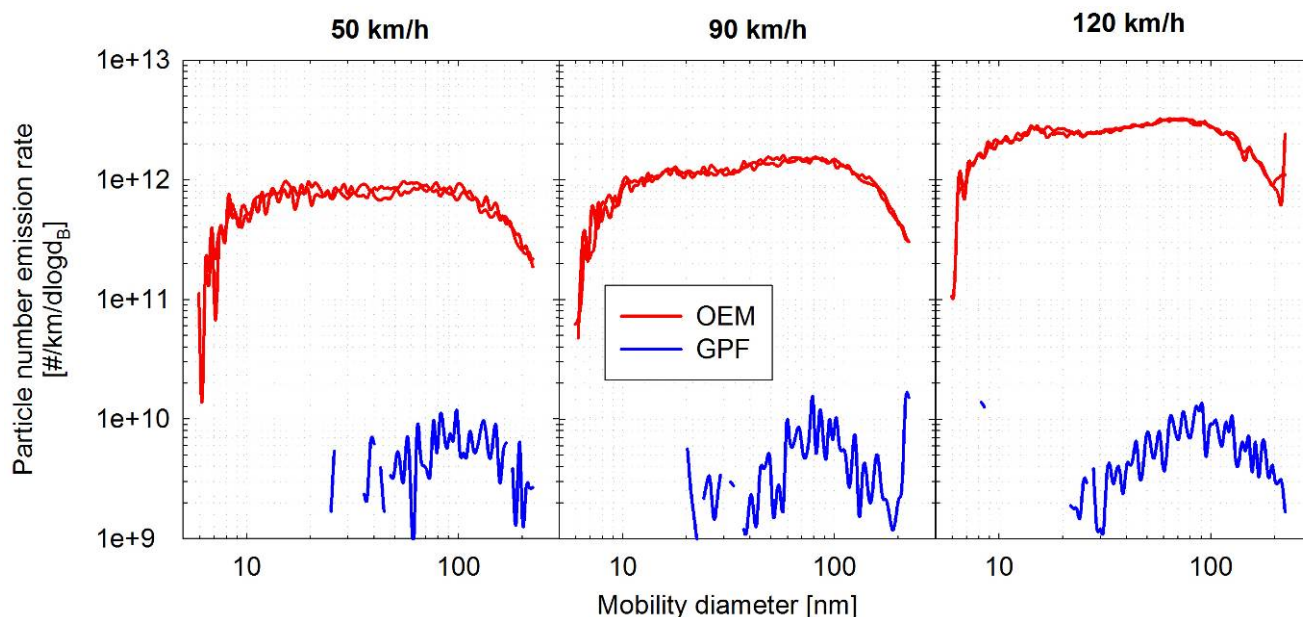


Figure 31: Number weighted mobility size distributions of the total particle population emitted by G-DI1 at 50 km/h, 90 km/h and 120 km/h with (red curves) and without (blue curves) GPF.

One of the concerns with respect to the installation of a GPF pertains to the underpressure introduced in the exhaust system that may potentially result in an increase of the CO<sub>2</sub> emissions. No CO<sub>2</sub> penalty could be identified with the GPF system tested at JRC. Actually the tests in which the GPF was retrofitted on the G-DI1 vehicle resulted in a slight but systematic reduction of the CO<sub>2</sub> emissions, which ranged from 0.9% at CADC urban to 3.5% over ECE (Figure 32). Similar benefits were reported by Mikulic et al. [40] from the installation of a GPF on a late technology stoichiometric G-DI tested over NEDC, and were attributed to increased internal Exhaust Gas Recirculation (EGR).

No indications of soot accumulation could be identified either in the particle number or the CO<sub>2</sub> emissions of the G-DI1 vehicle when retrofitted with the GPF. It is anticipated that the GPF was regenerating passively and therefore remained clean throughout the measurement campaign. The measured temperatures upstream of the GPF exceeded 500°C over most of the CADC test (Figure 33) and even reached 800°C over the motorway part. At the same time, the fuel cut-off during decelerations provided an oxygen rich environment that could initiate oxidation of accumulated soot.

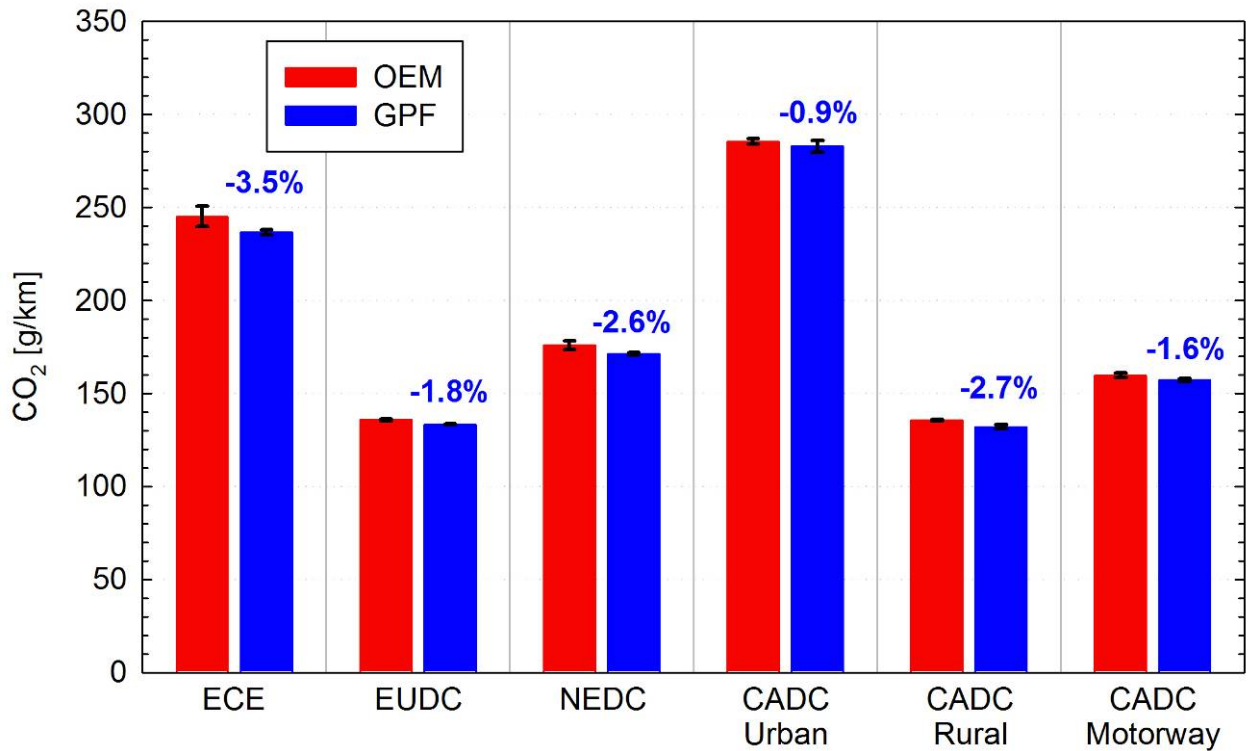


Figure 32: Carbon dioxide emissions of the G-D11 over the different cycles tested, with (blue bars) and without (red bars) GPF. The percentage figures indicate the relative difference in the CO<sub>2</sub> emissions resulting by the installation of the GPF. The error bars stand for  $\pm$  one standard error.

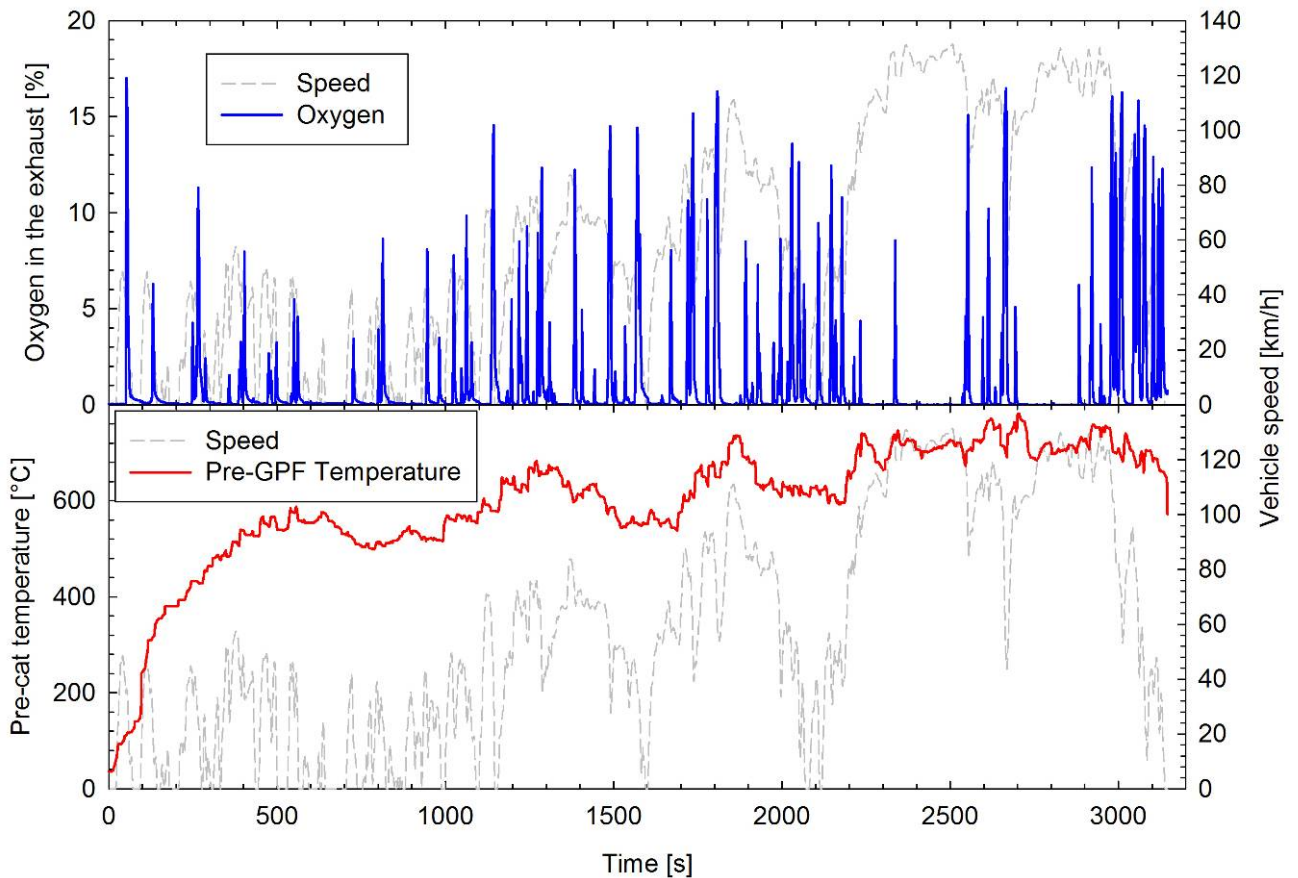


Figure 33: Measured exhaust temperature at the inlet of the GPF (bottom panel) and percentage concentration of oxygen in the exhaust (top panel) over a CADC test of the G-D11, when retrofitted with the GPF.

Another concern related to the application of GPF systems on G-DI vehicles, pertains to the feasibility of initiating active regeneration under urban conditions, especially for vehicles running stoichiometrically. Figure 34 shows the measured exhaust temperatures (downstream of the turbocharger) during NEDC tests of the G-DI1 at 22°C and -7°C. The measured data over the first 100 s of the cycle indicate that there exists the technology to reach exhaust temperatures in excess of 500°C even at speeds not exceeding 30 km/h and ambient temperatures of -7°C. In the tests at 22°C, the exhaust temperature reached 600°C within the first 60 s of operation, following which it dropped to sub-500°C levels as the catalyst was warmed up.

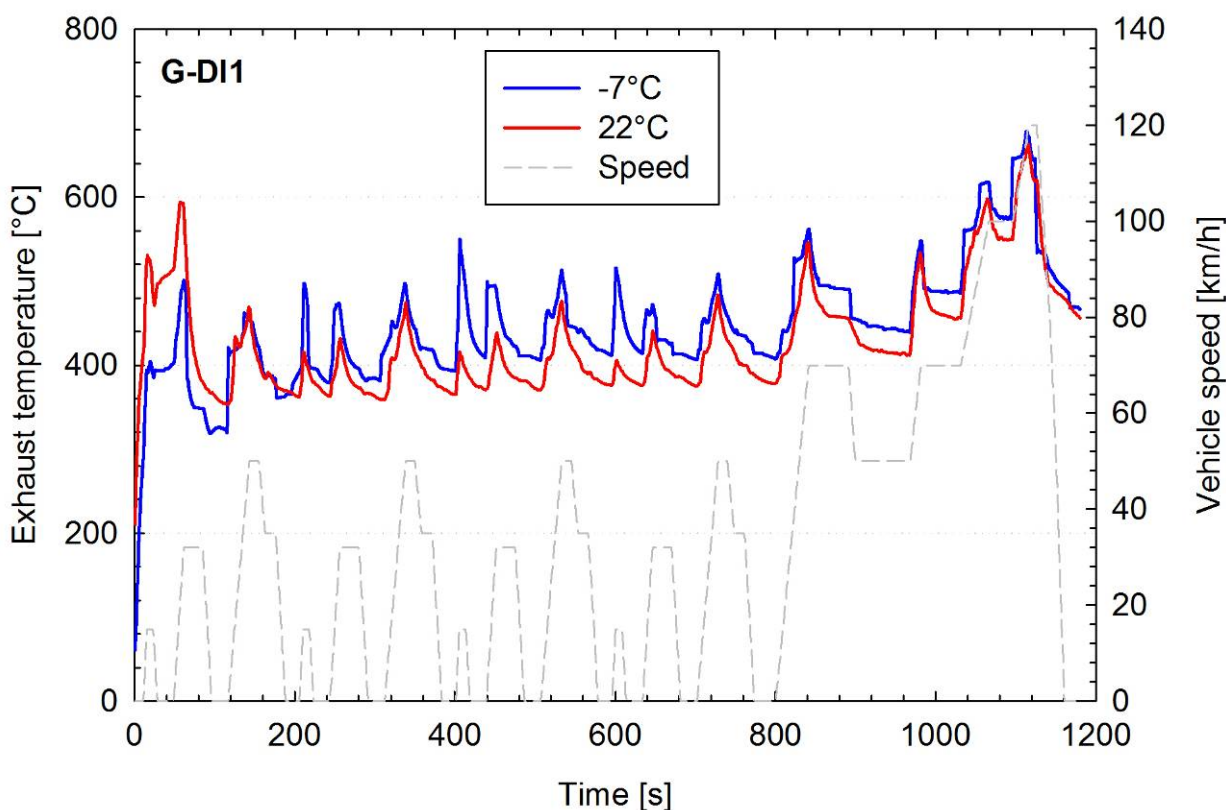


Figure 34: Measured exhaust temperature in the NEDC tests of the G-DI1 at 22°C (red lines) and -7°C (blue lines).

#### 4.6 G-DI/PFI emission performance

Figure 35 summarizes the particle number emissions of the G-DI/PFI vehicle over the different cycles at 22 and -7°C test cell temperatures. The emission levels of the particular vehicle were similar to conventional G-DIs only over the ECE phase of the NEDC, but once warmed up it emitted at a level around the diesel PN limit of  $6 \times 10^{11}$  #/km. Interestingly, the lower emission levels were accompanied with a shift of the distributions towards smaller sizes, with the fraction of non-volatile nanoparticles not detected by the PMP CPC lying in between of what observed for G-DI and PFI vehicles.

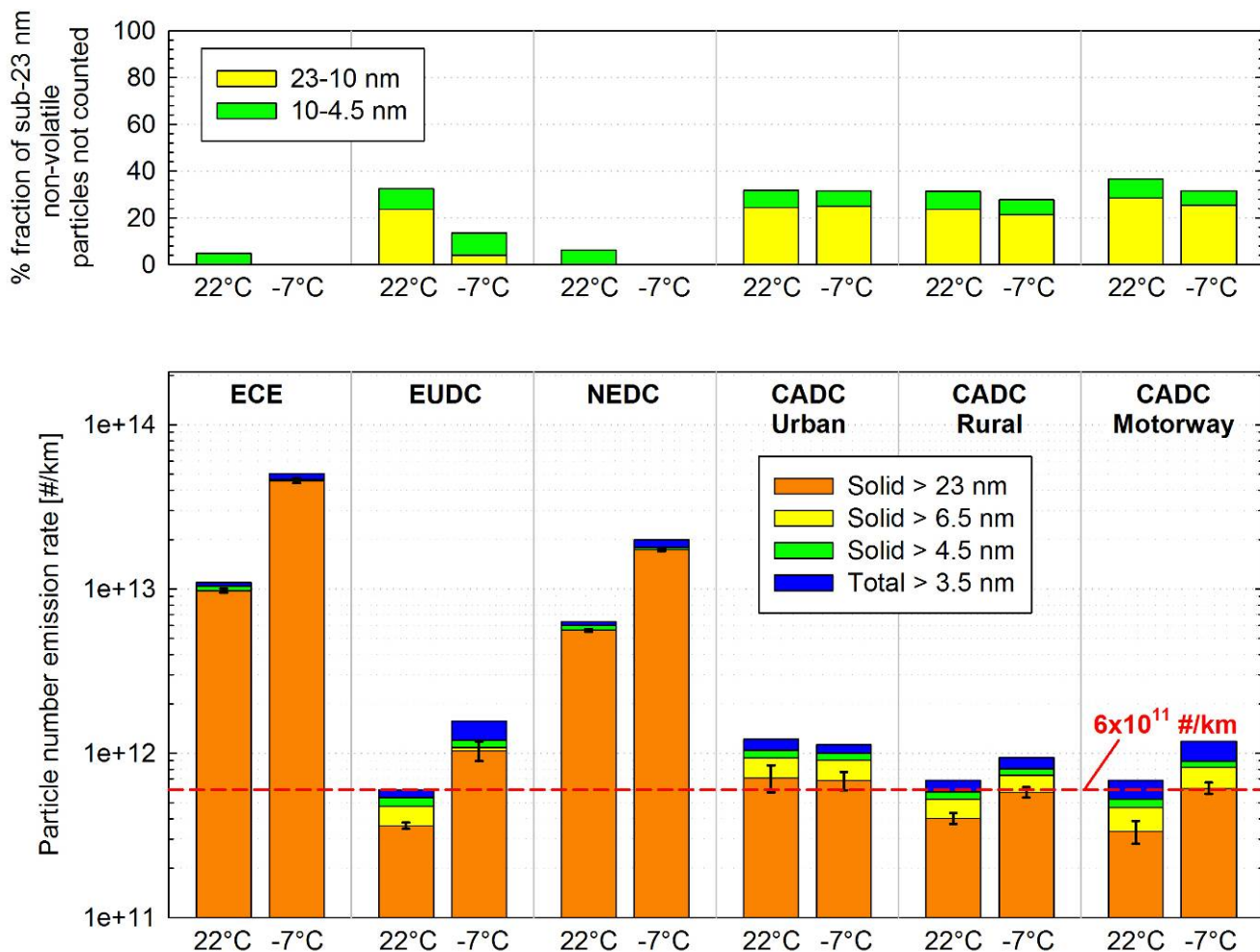


Figure 35: Average particle number emissions of the G-DI/PFI vehicle (bottom panel) and fraction of sub-23nm non-volatile particle counts not detected with the PMP CPC (top panel) over the NEDC and the CADC, at 22 and -7°C test cell temperature. Explanations as in Figure 6.

Figure 36 shows the real time particle number emissions traces recorded by the four different CPCs over one example NEDC test at 22°C. The emissions were found to gradually decrease over the cycle, with distance average emission rates of non-volatile particles > 23 nm ranging from  $3.4 \times 10^{13}$  #/km over the first ECE15 segment to  $1.8 \times 10^{12}$  #/km over the 4<sup>th</sup> ECE15 segment, reaching  $3.6 \times 10^{11}$  #/km over the EUDC part. This reduction in the particle number emissions was accompanied by a gradual shift of the distribution towards smaller sizes, as evident from the progressively larger differences between the particle counts determined by the PMP compliant CPC and those measured with the CPCs having a lower  $d_{50}$ .

Similar trends were observed in the NEDC tests performed at -7°C. In this case however, the sub-zero operation appeared to have affected the particle emissions over a prolonged period that also included the EUDC phase. The latter were found to be almost three times higher compared to the EUDC tests at 22°C.

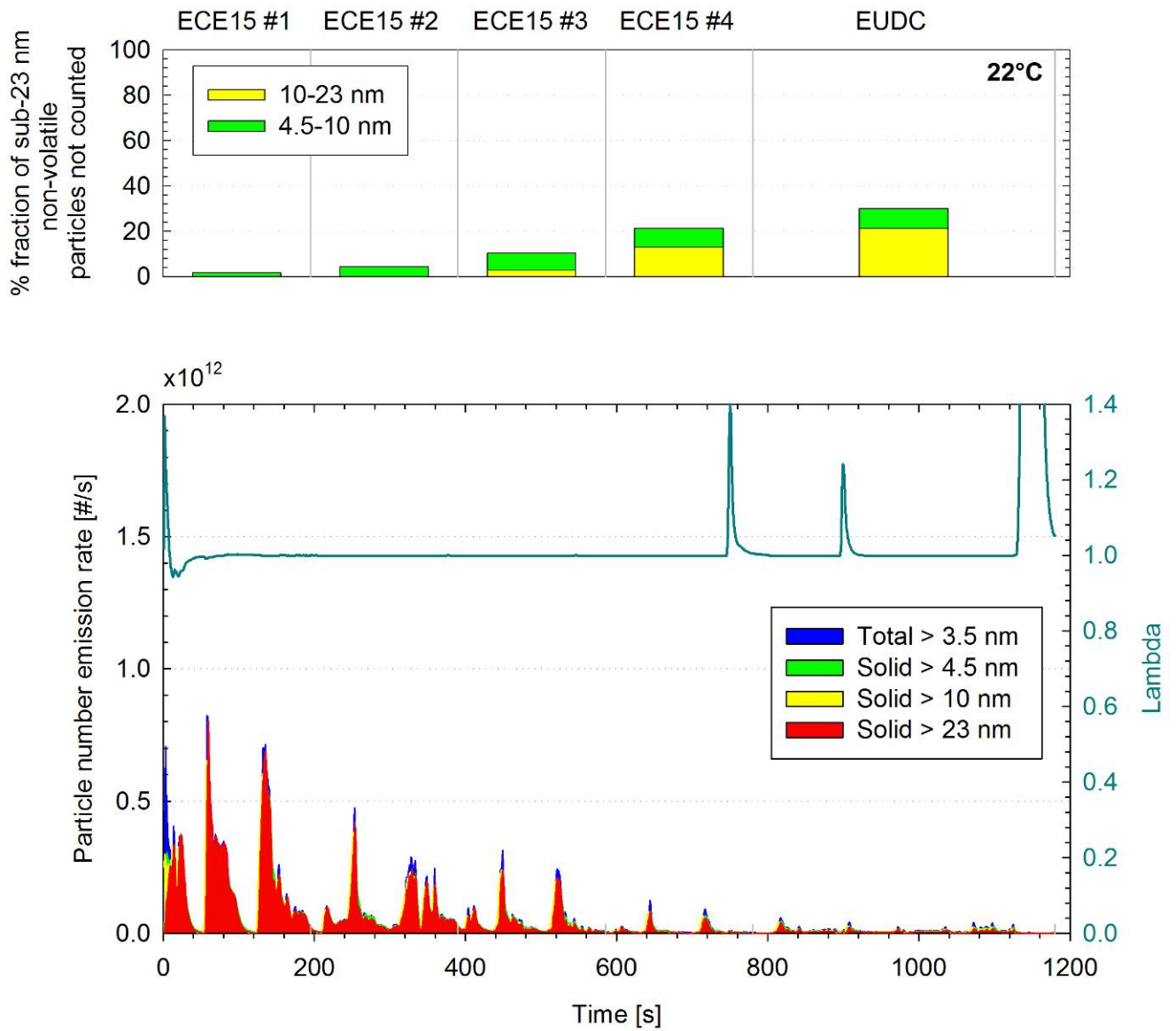


Figure 36: Particle number emission rates of the G-DI/PFI vehicle (bottom panel) and fraction of sub-23 nm non-volatile particle counts not detected with the PMP CPC (top panel) over the different segments of the NEDC at 22°C. The calculated lambda from the measured gaseous pollutants is also shown in the bottom panel (cyan line).

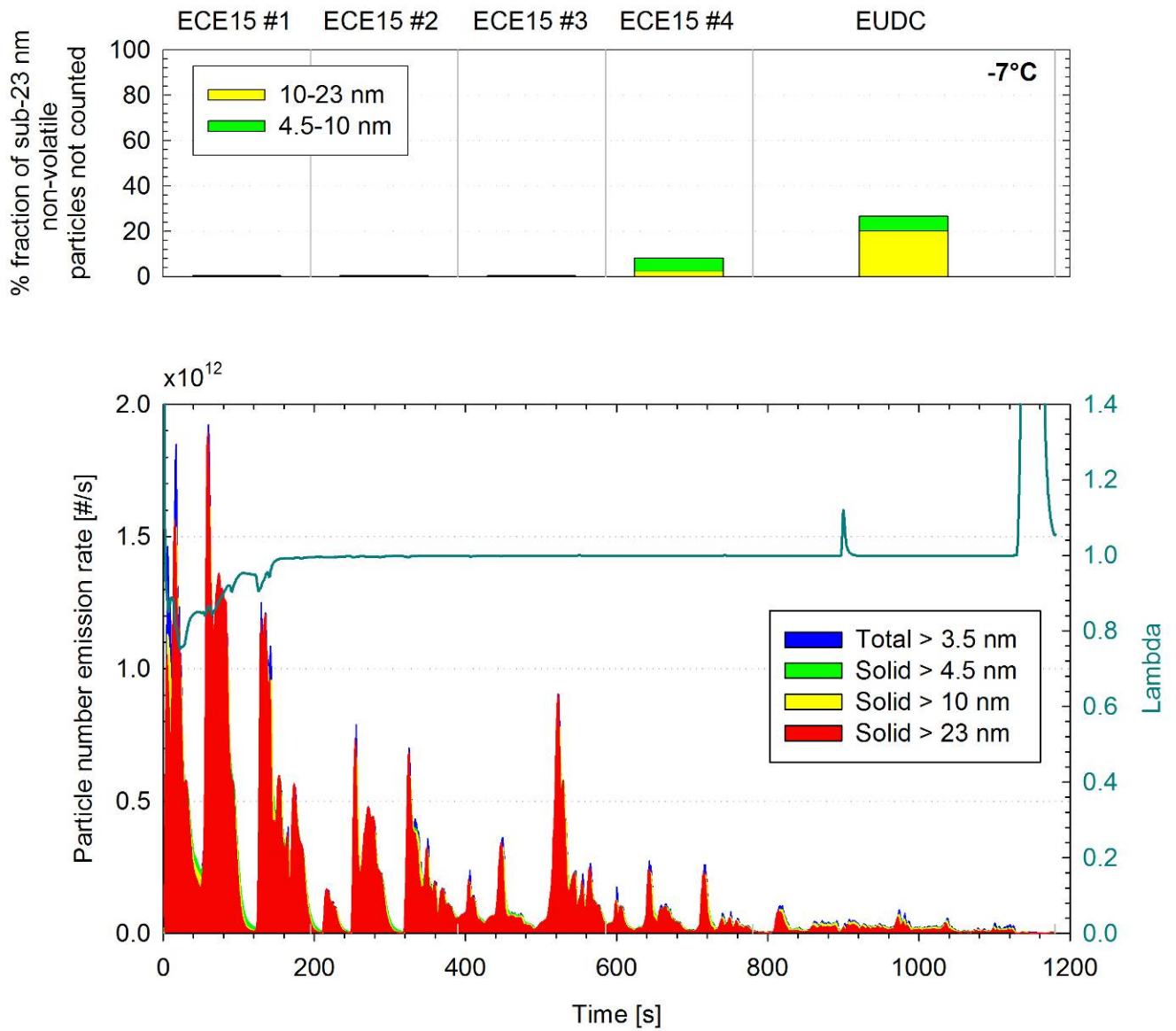


Figure 37: Particle number emission rates of the G-DI/PFI vehicle (bottom panel) and fraction of sub-23 nm non-volatile particle counts not detected with the PMP CPC (top panel) over the different segments of the NEDC at -7°C. The calculated lambda from the measured gaseous pollutants is also shown in the bottom panel (cyan line).

## 5 DISCUSSION & CONCLUSIONS

The present study investigated the suitability of the particle number measurement methodology, which is currently applicable for diesel vehicles, for the regulation of their gasoline counterparts. One of the main concerns pertains to the cut-off size of the CPC which is set at 23 nm in the regulation. In the case of diesels, the limit value necessitates the installation of very efficient wall particulate filters which have been shown to be equally or even more efficient in capturing sub-23 nm particles [41]. It is not clear however whether particulate filters will be required to control the particle emissions of gasoline vehicles. Port Fuel Injection (PFI) vehicles are generally found to emit below the diesel limit following the regulatory procedure [8], but were reported to exceed this threshold when a CPC with a lower cut-off size is employed [42]. Direct Injection Gasolines (G-DIs) were found to exceed the diesel limit by as much as one and a half orders of magnitude [8]. Wall flow particulate filters optimized for application on G-DI vehicles have already been developed [40, 43, 44], but advances in the combustion process also offer the potential for significant reductions in the particulate emissions of G-DIs [45, 46]. Some of the internal engine measures envisaged though, were found to reduce the size of the emitted particles [47], which under certain conditions even peaked below 23 nm [48].

To that end, the present study attempted to quantify the fraction of nano-sized non-volatile particles that are not detected by a PMP compliant CPC for a range of late technologies gasoline vehicles. The results indicated a distinct emission behavior of G-DI, PFI and DPF vehicles, that differed both in terms of the absolute levels but also with respect to the fraction of undetected nano-sized non-volatile particles. The latter was found to be around 20% (based on comparisons with a CPC@4.5) for three G-DI vehicles tested, but ranged between 40 and 70% for the two PFIs measured. Interestingly, a relatively large fraction of undetected nanosized was also observed for two late technology DPFs, ranging between 30 and 50%. To a large extent these differences originate from differences in the size distributions and the relatively blunt shape of the counting efficiency curve of PMP compliant CPCs.

Under conditions favouring nucleation mode formation in the CVS tunnel, excessive particle concentrations were detected by the low cut-off size CPCs, and especially the one with a  $d_{50}$  at 4.5 nm, that could exceed those of the PMP compliant CPC by up to one order of magnitude. However, the concentration of these nano-sized particles was found to decrease with increasing the dilution ratio in the first stage of the VPR, indicating that this is rather a volatile artifact possibly originating from re-nucleation of evaporated material downstream of the VPR.

Figure 38 gives an overview of the results collected over the NEDC at 22°C, where the nucleation mode potential was limited. Overall, the experimental data collected did not indicate excessive emissions of nano-sized particles, at least for current technology vehicles. Especially in the case of G-DIs, the regulated procedure was found to capture the majority of the emitted non-volatile particles (approximately 80%). The situation might change however in future technology G-DIs, especially if their particle number emissions will be controlled by internal engine measures, as there already exists evidence that such optimization may result in a shift of the particle size distributions towards smaller sizes [47, 48]. The emission performance of such advanced engines need to be assessed as soon as they become available. Yet, the present study provided evidence that the VPR systems are not suitable for the quantification of non-volatile particles at such small sizes due to volatile artifacts. More effective means for the treatment of the exhaust, like catalytic strippers [49, 50], may be required for such investigations.

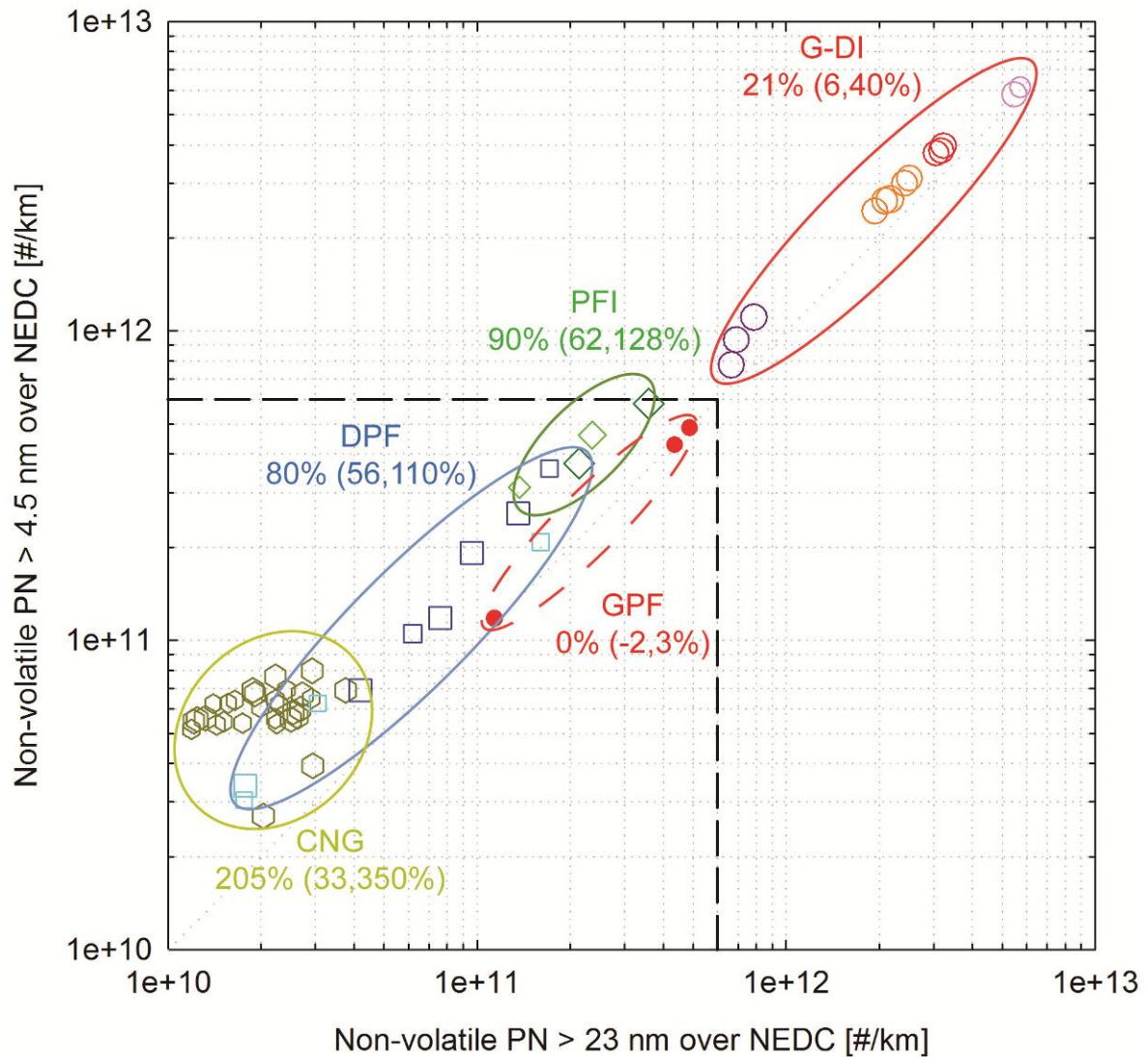


Figure 38: Comparison of the number emission rates of non-volatile particles measured with a PMP compliant CPC (horizontal axis) and a CPC with a  $d_{50}$  at 4.5 nm (vertical axis), over the NEDC. Different types of symbols correspond to different vehicle categories (circle for G-DIs, rhombus for PFI, squares for DPFs and hexagons for CNG) with different shades corresponding to different vehicles, and different sizes to different PCRFs (the larger the size the larger the dilution). The numbers indicate the average percentage difference between the CPC@4.5 and the PMP CPC results, followed by the minimum and maximum percentage differences in the parenthesis. The two dashed lines correspond to the  $6 \times 10^{11}$  #/km limit and are shown as a guideline.

The study also investigated some of the different available approaches to effectively control particle emissions from G-DI vehicles. These included the use of a GPF [40, 43, 44], the use of high ethanol fuel [20] and advanced engine concepts combining port and direct injection [51].

The GPF system investigated was found to be very efficient in the control of particle emissions under all driving conditions. Measured temperatures upstream of the underfloor GPF were found to exceed  $500^{\circ}\text{C}$  under all phases of the CADC test cycle, which is representative of typical European driving conditions. The fuel cut-off occurring during decelerations provided high concentrations of oxygen which at the elevated exhaust temperature could initiate oxidation of the accumulated soot. Furthermore no fuel consumption penalty could be identified under any condition tested. In fact, the results rather

suggested a small but systematic reduction (1-3.5%) in the CO<sub>2</sub> emitted, most probably due to increased internal Exhaust Gas Recirculation (EGR) [40].

Use of high ethanol content fuels (85% and 75%) on a flexi fuel G-DI vehicle was also found to be beneficial especially at high engine loads as well as during cold start operation. Reductions as high as 97% were observed in the particle number emissions over the motorway party of the CADC, in good agreement with what has been reported in the literature [20, 21]. Use of ethanol at such high levels, was also found to be beneficial in terms of CO<sub>2</sub> emissions, which were reduced by 6 to 8% depending on the driving conditions. Thus ethanol appears to offer a large global warming benefit through both black carbon and CO<sub>2</sub> reductions, that may actually be even higher if one considers the whole well to wheels path [52].

Finally, the engine utilizing both port and direct fuel injection also gave very promising results. Particles were mainly emitted under cold start operation but remained at around the diesel PN limit once the engine was warmed up. It needs to be emphasized that this particular vehicle was Euro 4 certified. Since no PM limit was applicable at this stage, it is expected that the engine was rather optimized for engine performance. Engine calibration towards low cold start particle emissions (e.g. increased rates of port fuel injection) could potentially offer significant advantages over the legislated NEDC test cycle.

One side-issue investigated was the effect of test cell temperature on the particulate emissions. The ambient temperature was found to affect only the cold start emissions of the gasoline vehicles. A shift in the test cell temperature from 25°C to 15°C, resulted in an average increase of the number of non-volatile particles emitted by PFI vehicles by 70% (PFI1) to 320% (PFI2). Similarly, a decrease in the temperature from 22°C to 15°C, resulted in 40%, on average, higher non-volatile particle number emissions from the single G-DI vehicle tested at both these conditions (GDI2).

The cold start effect was more pronounced over the NEDC tests at -7°C, where all three G-DIs emitted more than 5 to 6.5 times higher PM emissions. The non-volatile particle number emissions were also increased but to a lesser extent (2.3 to 3.1 times). This apparent inconsistency might reflect different volatile fractions or even changes in the size of the emitted particles. The latter is verified by the lower fraction of sub-23 nm particles counted during the sub-zero tests, which suggests larger emitted particle sizes under such operating conditions.

## 6 LIST OF SPECIAL TERMS AND ABBREVIATIONS

APC	AVL Particle Counter
CADC	Common Artemis Diving Cycle
CNG	Compressed Natural Gas
CO	Carbon Monoxide
CO <sub>2</sub>	Carbon Dioxide
CPC	Condensation Particle Counter
CPC@10	CPC having a nominal 50% counting efficiency at 10 nm
CPC@4.5	CPC having a nominal 50% counting efficiency at 4.5 nm
CPC_PMP	CPC complying with the European Regulations (d <sub>50</sub> at 23 nm)
CVS	Constant Volume Sampling
DG	Directorate General
DPF	Diesel Particulate Filter
E0	Gasoline fuel containing no ethanol
E5	5% Ethanol on Gasoline blend
E75	75% Ethanol on Gasoline blend
E85	85% Ethanol on Gasoline blend
EC	European Commission
ECE or UDC	Urban Driving Cycle (Part 1 of the NEDC driving cycle)
EGR	Exhaust Gas Recirculation
ENTR	Enterprise
EUDC	Extra Urban Driving Cycle (Part 2 of the NEDC driving cycle)
Euro #	European Emission Standard
FFV	Flexi Fuel Vehicle
G-DI	Gasoline Direct Injection
GPF	Gasoline Particulate Filter
H <sub>2</sub>	Hydrogen

HC	Hydrocarbon
ILCE_HD	Heavy Duty Inter-Laboratory Correlation Exercise
ILCE_LD	Light Duty Inter-Laboratory Correlation Exercise
JRC	Joint Research Centre
NEDC	New European Driving Cycle
NO <sub>x</sub>	Oxides of Nitrogen (NO & NO <sub>2</sub> )
O <sub>2</sub>	Oxygen
OEM	Original Equipment Manufacturer
PFI	Port Fuel Injection
PM	Particulate Matter mass
PMP	Particle Measurement Programme
PN	Particle Number
TWC	Three Way Catalyst
UN-ECE GRPE	United Nations Economic Commission for Europe Working Party on Pollution and Energy
VELA	Vehicles Emission Laboratory
VPR	Volatile Particle Removers

## REFERENCES

---

1 Vouitsis E., Ntziachristos L. and Samaras Z. (2003). Particulate matter mass measurements for low emitting diesel powered vehicles: what's next? *Progress in Energy and Combustion Science*, 29: 635-672.

2 WHO (2005). *Air Quality Guidelines for Particulate Matter, Ozone, Nitrogen Dioxide and Sulfur Dioxide Global Update 2005*. World Health Organization Copenhagen, Denmark.

3 Andersson J., Giechaskiel B., Muñoz-Bueno R., Sandback E. And Dilara P. (2007). Particle Measurement Programme (PMP) Light-Duty Inter-Laboratory Correlation Exercise (ILCE\_LD) Final Report. EUR 22775 EN, [http://ies.jrc.ec.europa.eu/uploads/fileadmin/Documentation/Reports/Emissions\\_and\\_Health/EUR\\_2006-2007/EUR\\_22775\\_EN.pdf](http://ies.jrc.ec.europa.eu/uploads/fileadmin/Documentation/Reports/Emissions_and_Health/EUR_2006-2007/EUR_22775_EN.pdf)

4 Agreement concerning the adoption of uniform technical prescriptions for wheeled vehicles, equipment and part which can be fitted and/or be used on wheeled vehicles and the conditions for reciprocal recognition of approvals granted on the basis of these prescriptions. <http://www.unece.org/trans/main/wp29/wp29regs/r083r3a2e.doc>

5 Commission Regulation (EC) No 692/2008, 18 July 2008, "Implementing and amending Regulation (EC) No 715/2007 of the European Parliament and of the Council on type-approval of motor vehicles with respect to emissions from light passenger and commercial vehicles (Euro 5 and Euro 6) and on access to vehicle repair and maintenance information". <http://eur-lex.europa.eu/LexUriServ/LexUriServ.do?uri=OJ:L:2008:199:0001:0136:EN:PDF>

6 Regulation (EC) No 715/2007 of the European Parliament and of the Council of 20 June 2007, "On type approval of motor vehicles with respect to emissions from light passenger and commercial vehicles (Euro 5 and Euro 6) and on access to vehicle repair and maintenance information". <http://eur-lex.europa.eu/LexUriServ/LexUriServ.do?uri=OJ:L:2007:171:0001:0016:EN:PDF>

7 Official Journal of the European Union, "Communication on the application and future development of Community legislation concerning vehicle emissions from light-duty vehicles and access to repair and maintenance information (Euro 5 and 6)", 2008/C 182/08, <http://eur-lex.europa.eu/LexUriServ/LexUriServ.do?uri=OJ:C:2008:182:0017:0020:EN:PDF>

8 A. Mamakos and C. Dardiotis. (2011). Assessment of Particle Number Limits for Petrol Vehicles. JRC Report. Available at: [http://circa.europa.eu/Public/irc/enterprise/automotive/library?l=/mveg\\_vehicle\\_emissions/107th\\_january\\_2011/2\\_0110124\\_circapdf/EN\\_1.0\\_&a=d](http://circa.europa.eu/Public/irc/enterprise/automotive/library?l=/mveg_vehicle_emissions/107th_january_2011/2_0110124_circapdf/EN_1.0_&a=d)

9 A. Mamakos, C. Dardiotis, A. Marotta, G. Martini, U. Manfredi, R. Colombo, M. Sculati, P. Le Lijour, G. Lanappe. (2011). Particle Emissions from a Euro 5a Certified Diesel Passenger Car. JRC Scientific and Technical Report. EUR 24855 EN. Available for download at: [http://publications.jrc.ec.europa.eu/repository/bitstream/111111111/22040/1/jrc\\_report\\_particle\\_emissions\\_from\\_a\\_euro5a\\_diesel\\_vehicle.pdf](http://publications.jrc.ec.europa.eu/repository/bitstream/111111111/22040/1/jrc_report_particle_emissions_from_a_euro5a_diesel_vehicle.pdf)

10 Directive 2009/30/EC of the European Parliament and of the Council of 23 April 2009 amending Directive 98/70/EC as regards the specifications of petrol, diesel and gas oil and introducing a mechanism to monitor and reduce greenhouse gas emissions and amending Council Directive 1999/32/EC as regards the specification of fuel used by inland waterway vessels and repealing Directive 93/12/EEC. Available for download at: <http://eur-lex.europa.eu/LexUriServ/LexUriServ.do?uri=OJ:L:2009:140:0088:0113:EN:PDF>

11 André M. (2004). The ARTEMIS European Driving Cycles for Measuring Car Pollutant Emissions. *Science of the Total Environment*, 334-335:73-84.

12 United Nations, Economic Commission for Europe, ECE/TRANS/WP.29/2009/57, Regulation No 83, "Uniform Provisions Concerning the Approval of Vehicles with Regard to the Emission of Pollutants According to Engine Fuel Requirements", 2009

- 
- 13 Hueglin C., Scherrer L., Burtscher H., "An accurate continuously adjustable dilution system (1:10 to 1:104) for submicron aerosols", *Journal of Aerosol Science* 28 (6), pp. 1049-1055, 1997
- 14 Kasper M., "The number concentration of non-volatile particles – design study for an instrument according to the PMP recommendations", *SAE Paper 2004-01-0960*, 2004
- 15 Ntziachristos L., Giechaskiel B., Pistikopoulos P., Samaras Z., "Comparative assessment of two different sampling systems for particle emission type-approval measurements", *SAE Paper 2005-01-0198*, 2005
- 16 Giechaskiel B., Cresnoverh M., Jörgl H. and Bergmann A. (2010). Calibration and Accuracy of a Particle Number Measurement System. *Measurement Science and Technology*, 21 045102.
- 17 Giechaskiel B. and Drossinos Y. (2010). Theoretical Investigation of Volatile Removal Efficiency of Particle Number Measurement Systems. *SAE Technical Paper 2010-01-1304*
- 18 Mamakos A., Giechaskiel B., Drossinos Y., Lesueur D., Martini G. and Krasenbrink A. (2011). Calibration and Modeling of PMP compliant Condensation Particle Counters. *JRC Scientific and Technical Report, EUR 25145 EN*.
- 19 United Nations, Economic Commission for Europe, ECE/TRANS/WP.29/2009/57, Regulation No 83, "Uniform Provisions Concerning the Approval of Vehicles with Regard to the Emission of Pollutants According to Engine Fuel Requirements", 2009
- 20 Szybist J., Youngquist A., Barone T., Storey J., Moore W., Foster M. and Confer K. (2011). Ethanol Blends and Engine Operating Strategy Effects on Light-Duty Spark-Ignition Engine Particle Emissions. *Energy & Fuels*, 25: 4977–4985.
- 21 Lee J., Patel R., Schonborn A., Ladommatos N. and Bae C. (2009). Effect of Biofuels on Nanoparticle Emissions from Spark- and Compression-ignited Single-cylinder Engines with Same Exhaust Displacement Volume. *Energy & Fuels*, 23:4363-4369.
- 22 Giechaskiel B., Wang X., Horn H.-G., Spielvogel J., Gerhart C., Southgate J., Jing L., Kasper M., Drossinos Y. and Krasenbrink A. (2009). Calibration of Condensation Particle Counters for Legislated Vehicle Number Emission Measurements. *Aerosol Science and Technology*, 43:1164–1173.
- 23 Wang X., Caldow R., Sem G., Hama N. and Sakura H. (2010). Evaluation of a Condensation Particle Counter for Vehicle Emission Measurement: Experimental Procedure and Effects of Calibration Aerosol Material. *Journal of Aerosol Science*, 41: 306-318.
- 24 Giechaskiel B., Wang X., Gilliland D. and Drossinos Y. (2011). The Effect of Particle Chemical Composition on the Activation Probability in butanol Condensation Particle Counters. *Journal of Aerosol Science*, 42: 20-37.
- 25 Ntziachristos L., Mamakos A., Samaras Z., Mathis U., Mohr M., Thompson N., Strandling R., Forti L. and de Serves C. (2004). Overview of the European "Particulates" Project on the Characterization of Exhaust Particulate Emissions for Road Vehicles: Results for Light Duty Vehicles. *SAE Technical Paper 2004-01-1985*
- 26 Mohr M., Forss A.-M. and Lehmann U. (2006). Particle Emissions from Diesel Passenger Cars Equipped with a Particle Trap in Comparison to Other Technologies. *Environmental Science and Technology* 40: 2375-2383.
- 27 Alger T., Gingrich J., Khalek I. and Mangold B. (2010). The Role of EGR in PM Emissions from Gasoline Engines. *SAE Technical Paper 2010-01-0353*.
- 28 Khalek I., Bougher T. and Jetter J. (2010). Particle Emissions from a 2009 Gasoline Direct Injection Engine Using Different Commercially Available Fuels. *SAE Technical Paper 2010-01-2117*.
- 29 Hedge M., Weber P., Gingrich J., Alger T. and Khalek I. (2011). Effect of EGR on Particle Emissions from a GDI Engine. *SAE Technical Paper 2011-01-0636*.

---

30 Swanson J. and Kittelson D. (2010). Evaluation of Thermal Denuder and Catalytic Stripper Methods for Solid Particle Measurements. *Journal of Aerosol Science*, 41:1113-1122.

31 Giechaskiel B., Munoz-Bueno R., Rubino L., Manfredi U., Dilara P., De Santi G. and Andersson J. (2007). Particle Measurement Programme (PMP): Particle Size and Number Emissions Before, During and After Regeneration Events of a Euro 4 DPF Equipped Light-Duty Diesel Vehicle, SAE Technical Paper 2007-01-1944

32 Ciambelli P., Palma V., Russo P. and Vaccaio, S. (2005). Issues on Soot Removal from Exhaust Gases by Means of Radial Flow Ceramic Traps, *Chemical Engineering Science* 60:1619-1627.

33 Braisher M., Stone R. and Price, P. (2010). Particle Number Emissions from a Range of European Vehicles, SAE Technical Paper 2010-01-0786.

34 Tao T., Cutler W., Voss K. and Wei Q. (2003). New Catalyzed Cordierite Diesel Particulate Filters for Heavy Duty Engine Applications. SAE Technical Paper 2003-01-3166.

35 Khalek I., Kittelson D. and Brear F. (2000) Nanoparticle growth during dilution and cooling of diesel exhaust: Experimental investigation and theoretical assessment. SAE technical paper 2000-01-0515.

36 Vouitsis E., Ntziachristos L. and Samaras Z. (2005). Modelling of diesel exhaust aerosol during laboratory sampling. *Atmospheric Environment*, 39:1335–1345.

37 Swanson J., Kittelson D., Watts W., Gladis D. and Twigg M. (2009). Influence of storage and release on particle emissions from new and used CRTs. *Atmospheric Environment*, 43:3998–4004

38 Ordonez S., Hurtado P. and Diez F. (2005). Methane Catalytic Combustion over Pd/Al<sub>2</sub>O<sub>3</sub> in Presence of Sulphur Dioxide: Development of a Regeneration Procedure. *Catalysis Letters*, 100: 27-34.

39 Liu P. and Deshler T. (2003). Causes of Concentration Differences Between a Scanning Mobility Particle Sizer and a Condensation Particle Counter. *Aerosol Science and Technology* 37: 916-923

40 Mikulic I., Koelman H., Majkowski S. and Vosejпка P. (2010). A Study about Partilce Filter Application on a State-of-the-Art Homogeneous Turbocharged 2L DI Gasoline Engine. *Aachener Kolloquium Fahrzeug- und Motorentechnik 2010*.

41 De Fillipo A. and Maricq M. (2008). Diesel Nucleation Mode Particles: Semivolatile or Solid?, *Environmental Science and Technology* 42:7957-7962.

42 Schreiber D., Forss A.-M., Mohr M. and Dimopoulos P. (2007). Particle Characterisation of Modern CNG, Gasoline and Diesel Passenger Cars. SAE Technical Paper 2007-24-0123.

43 Zhan R., Eakle S.T. and Weber P. (2010). Simultaneous Reduction of PM, HC, CO and NO<sub>x</sub> Emissions from a GDI Engine. SAE Technical Paper 2010-01-0365

44 Saito C., Nakatani T., Miyairi Y., Yuuki K., Makino M., Kurachi H., Heuss W., Kuki T., Furuta Y., Kattouah P. and Vogt C.-D. (2011). New Particulate Filter Concept to Reduce Particle Number Emissions. SAE Technical Paper 2011-01-0814.

45 Piock W., Hoffmann G., Berndorfer A., Salemi P. and Fusshoeller B. (2010). Strategies Towards Meeting Future Particulate Matter Emission Requirements in Homogeneous Gasoline Direct Injection Engines. SAE Technical Paper 2011-01-1212.

46 Dobes T., Fraidl G., Hollerer P., Kapus P., Ogris M. and Reiner M. (2011). Measures to Comply with Future Particulate Number Standards with GDI Engines. 32nd International Vienne Motor Symposium. 05-06 May 2011.

47 Barone T. L., Storey J. M., Youngquist A. D. and Szybist J. P. (2011). An Analysis of Direct-Injection Spark-Ignition (DISI) Soot Morphology. *Atmospheric Environment*, doi: 10.1016/j.atmosenv.2011.11.047

---

48 Hedge M., Weber P., Gingrich J., Alger T. and Khalek I. (2011). Effect of EGR on Particle Emissions from GDI Engine. SAE Technical Paper 2011-01-0636.

49 Swanson J. and Kittelson D. (2010). Evaluation of thermal denuder and catalytic stripper methods for solid particle measurements. *Journal of Aerosol Science*, 41:113-1122

50 Khalek I. and Bougher T. (2011). Development of a Solid Exhaust Particle Number Measurement System Using a Catalytic Stripper Technology. SAE Technical Paper 2011-01-0635.

51 Heiduk T., Dornhöfer R., Eiser A., Grigo M., Pelzer A. and Wurms R. The New Engine Generation of R4 TFSI from Audi. (2011). 32nd International Vienna Motor Symposium

52 Edwards R., Larive J. F. and Beziat J. C. (2011). Well-to-wheels Analysis of Future Automotive Fuels and Powertrains in the European Context. Version 3c. JRC Scientific and Technical Report EUR 24952 EN.

European Commission

EUR 25382 EN – Joint Research Centre – Institute for Energy and Transport

Title: Physical Characterization of Exhaust Particle Emissions from Late Technology Gasoline Vehicles.

Author(s): Athanasios Mamakos, Urbano Manfredi

Editor(s): Giorgio Martini, Adolfo Perujo, Alessandro Marotta

Luxembourg: Publications Office of the European Union

2012 – 56 pp. – 21.0 x 29.7 cm

EUR – Scientific and Technical Research series – ISSN 1831-9424 (online), ISSN 1018-5593 (print)

ISBN 978-92-79-25312-6 (pdf)

ISBN 978-92-79-25313-3 (print)

doi:10.2788/32371

## Abstract

The study assesses the feasibility of introducing the regulated particle number measurement procedure for the regulation of gasoline vehicles, focusing on the established cut-off size of 23 nm. A range of late technology gasoline vehicles were tested under regulated and unregulated test conditions. The results indicated a distinct emission behavior of Direct Injection Gasolines (G-DI), Port Fuel Injection gasolines (PFI) and Diesels equipped with Particulate Filters (DPF), that differed both in terms of the absolute levels but also with respect to the fraction of undetected nano-sized non-volatile particles. The latter was found to be around 20% (based on comparisons with a Condensation Particle Counter (CPC) having a 50% cut-off size at 4.5 nm) for three G-DI vehicles tested, but ranged between 40 and 70% for the two PFIs measured. Interestingly, a relatively large fraction of undetected nanosized was also observed for two late technology DPFs, ranging between 30 and 50%. To a large extent these differences originate from differences in the size distributions and the relatively blunt shape of the counting efficiency curve of PMP compliant CPCs.

Under conditions favouring nucleation mode formation in the dilution tunnel, excessive particle concentrations were detected by the low cut-off size CPCs, and especially the one with a  $d_{50}$  at 4.5 nm, that could exceed those of the PMP compliant CPC by up to one order of magnitude. However, the concentration of these nano-sized particles was found to decrease with increasing the dilution ratio in the first stage of the Volatile Particle Remover (VPR), indicating that this is rather a volatile artifact possibly originating from re-nucleation of evaporated material downstream of the VPR.

The study also investigated the potential offered by a range of available approaches to effectively control particle emissions from G-DIs. These included the use of a Gasoline Particulate Filter (GPF), the introduction of ethanol in the fuel but also an advanced engine concept combining port and direct fuel injection. The GPF system was found to very efficient in controlling particle number emissions under all driving conditions, having no visible impact on carbon dioxide emissions. The use of fuel with hi-ethanol content (75-85%) was also found to be beneficial especially at high engine loads (up to 97% reduction of non-volatile particle numbers) and during cold start operation (up to 70% reduction). The tests with the “hybrid” G-DI-PFI vehicle indicated that there exists the potential for significant reduction of PM formation through engine measures. The non-volatile particle number emissions of this vehicle remained below the diesel limit over all hot start tests.

As the Commission's in-house science service, the Joint Research Centre's mission is to provide EU policies with independent, evidence-based scientific and technical support throughout the whole policy cycle.

Working in close cooperation with policy Directorates-General, the JRC addresses key societal challenges while stimulating innovation through developing new standards, methods and tools, and sharing and transferring its know-how to the Member States and international community.

Key policy areas include: environment and climate change; energy and transport; agriculture and food security; health and consumer protection; information society and digital agenda; safety and security including nuclear; all supported through a cross-cutting and multi-disciplinary approach.